INTERFERENCE-MINIMIZED MULTIPATH ROUTING WITH CONGESTION CONTROL IN WIRELESS SENSOR NETWORK FOR MULTIMEDIA STREAMING

TEO JENN YUE BUGSY

(B.Eng.(Hons.), NUS)

A THESIS SUBMITTED

FOR THE DEGREE OF MASTER OF ENGINEERING

DEPARTMENT OF ELECTRICAL & COMPUTER ENGINEERING

NATIONAL UNIVERSITY OF SINGAPORE

2007

Acknowledgements

My sincere thanks go to my supervisor, Assistant Professor Ha Yajun. I have enjoyed two fulfilling years doing research under his supervision. He has imparted to me knowledge that is both practical and invaluable to my future endeovers. He has also gone beyond his duties of a supervisor to act as a mentor and friend.

I would also like to thank my co-supervisor, Associate Professor Tham Chen Khong. He has given me valuable advice and insight to the domain of wireless ad-hoc networking. Without his advice and suggestions, this thesis would not have been possible.

I would also like to express my gratitude to my sponsoring company, DSO National Laboratories. The DSO Postgraduate Scholarship has presented me the opportunity to obtain my Masters degree and also upgrade my technical knowledge and skills. In addition, I would like to thank my bosses and colleagues in DSO, who have been encouraging and supportive during my studies.

In addition, I would like to thank Chee Seng and Say Huan for helping me in many ways.

Last but not least, I would like to give special thanks to my family, friends and anyone who is not mentioned here but had helped me in one way or another.

Contents

Abstract

Multimedia streaming in Wireless Sensor Network (WSN) is required for future military applications like battlefield surveillance to provide high-quality information of hot spots. Although recent advances have enabled large-scale WSN to be deployed supported by high-bandwidth backbone network for multimedia streaming, the single-channel and energy-constrained WSN still remains the bottleneck due to the low-rate radios used by the sensor nodes and the effects of wireless interferences that severely limit throughput. Therefore, it is crucial to consider the effects of wireless interferences when using multipath load balancing.

Multipath load balancing can be used to increase throughput, but simply using link- or node-disjoint shortest paths is not sufficient to guarantee any throughput gains. In order for multipath load balancing to be effective, shortest paths that are physically separated (i.e. maximally zone-disjoint shortest paths) need to be discovered and used, so as to minimize the effects of wireless interferences. However, discovering maximally zone-disjoint shortest paths without network-wide localization support or directional antennas is challenging and the problem is worse when nodes

interfere beyond their communication ranges.

In this thesis, three contributions are made: First, a modeling technique for multipath load balancing is proposed. The technique captures the effects of both inter- and intra-path wireless interferences using conflict graphs, without having to assume that nodes do not interfere beyond their communication ranges. A metric that can be used to evaluate the quality of a path-set for multipath load balancing is then derived from the conflict graphs.

Second, a heuristics-based Interference Minimized Multipath Routing (I2MR) protocol is proposed. The protocol increases throughput by discovering and using maximally zone-disjoint shortest paths for load balancing, while requiring minimal localization support and incurring low routing overheads. Furthermore, directional antennas are not used and nodes are assumed that they may interfere up to twice their communication ranges.

Third, a congestion control scheme for I2MR is proposed. The scheme further increases throughput by dynamically reducing the load-rate of the source when long-term congestions are detected along the active paths used for load balancing. The active paths are eventually loaded at the highest possible rate that can be supported, so as to minimize long-term path congestions.

Lastly, the proposed path-set evaluation technique is validated using GloMoSim simulations. The proposed I2MR protocol with congestion control is also evaluated

using simulations by comparing with the unipath Ad-hoc On-demand Distance Vector (AODV) protocol and the multipath Node Disjoint Multipath Routing (NDMR) protocol. Simulation results show that I2MR with congestion control achieves on average 230% and 150% gains in throughput over AODV and NDMR respectively, and consumes comparable or at most 24% more energy than AODV but up to 60% less energy than NDMR.

List of Figures

List of Tables

List of Abbreviations

AO	AREA OF OPERATIONS
AODV	AD-HOC ON-DEMAND DISTANCE VECTOR
BER	BIT ERROR RATE
BZP	BROADCAST ZONE-MARKER POTENTIAL
CBR	CONSTANT BIT RATE
DCF	DISTRIBUTED COORDINATION FUNCTION
DSR	DYNAMIC SOURCE ROUTING
EO	ELECTRO-OPTIC
GLOMOSIM	GLOBAL MOBILE SYSTEMS SIMULATOR
I2MR	INTERFERENCE-MINIMIZED MULTIPATH ROUTING
IZ	INTERFERENCE ZONE
LC-ARQ	LAYERED-CODING WITH SELECTIVE ARQ
MAC	MEDIUM ACCESS CONTROL
MDC	MULTIPLE DESCRIPTIONS CODING
MDMC	MULTIPLE DESCRIPTIONS MOTION COMPENSATION

NDMR NODE-DISJOINT MULTIPATH ROUTING

RREP ROUTE REPLY

RREQ ROUTE REQUEST

RSSI RECEIVED SIGNAL STRENGTH INDICATION

SH SECTOR HEAD

SNR SIGNAL TO NOISE RATIO

UAV UNMANNED AERIAL VEHICLE

WSN WIRELESS SENSOR NETWORK

Chapter 1

Introduction

Chapter 1 is organized as follow: Section 1.1 describes the targeted WSN application scenario and network architecture. Section 1.2 describes current limitations. Section 1.3 describes the proposed solutions. Section 1.4 describes the organization of this thesis.

1.1 WSN Application and Network Architecture

Multimedia streaming in Wireless Sensor Network (WSN) is required for future military applications like battlefield surveillance to provide high-quality information of battlefield hot spots. Recent advances allow large-scale WSN to be deployed supported by high-bandwidth backbone network for multimedia streaming. Initially,

large quantities of low-power sensor nodes are airdropped into the Area of Operations (AO), forming a ground WSN. During periods of high conflict, additional sensor nodes with Electro-Optic (EO) devices, capable of networking with the existing ground WSN, will be hand-deployed by soldiers to monitor strategic areas within the AO. Unmanned Aerial Vehicles (UAVs) can be deployed to provide the high-bandwidth backbone network to relay information collected from the ground WSN to a remote command center. Higher-power gateway nodes that are capable of linking up the ground WSN and the UAV backbone network will be airdropped in areas with direct UAV coverage. Not all areas within the AO have direct UAV coverage due to overhead foliage. A possible deployment scenario is as shown in Figure 1.1.

When enemy targets activate the low-power sensor nodes, they will in turn activate the sensor nodes with EO devices to capture images or low-resolution videos of the targets. This information needs to be transmitted in a near real-time manner to the remote command center via the UAV network. As the sensor nodes capturing the target information may not be able to communicate directly with the gateway nodes, target information may be required to be relayed in a multi-hop manner through the low-power ground WSN, as shown in Figure 1.2. It is currently assumed that the bandwidth of the UAV backbone network is sufficient and will not be the bottleneck.

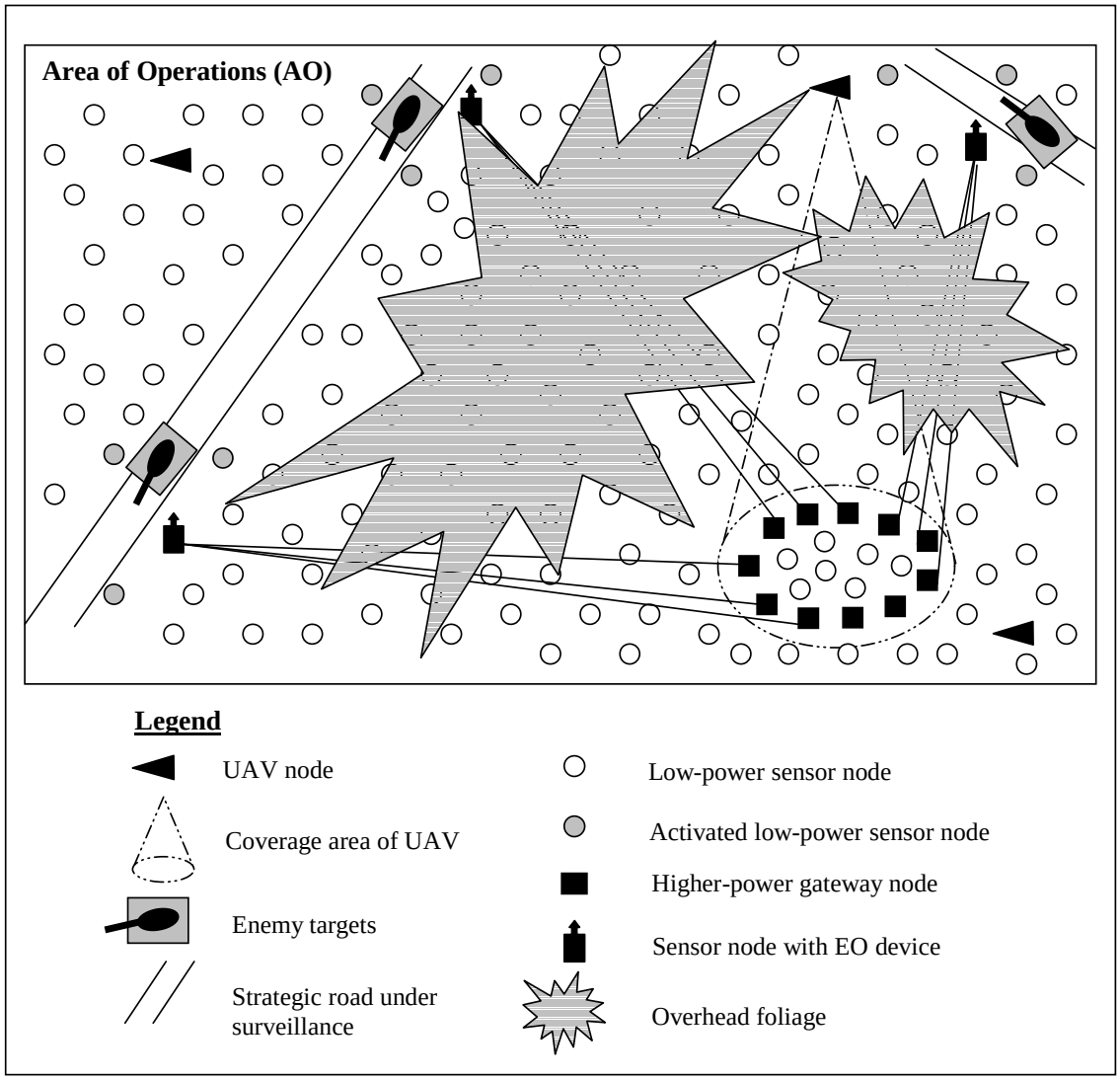

Figure 1.1: Possible deployment scenario.

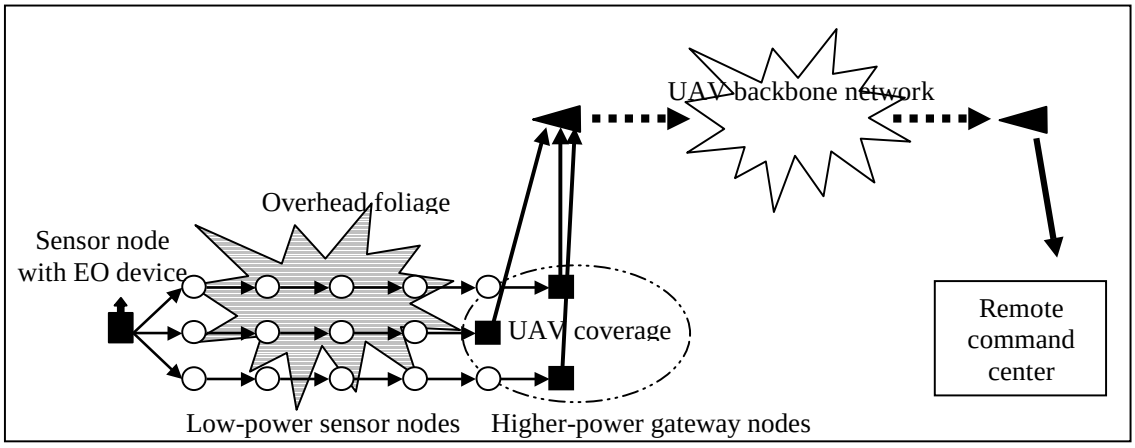

Figure 1.2: Relaying target information to remote command center.

1.2 Current Limitations

Although a high-bandwidth backbone network can be deployed to support the WSN, multimedia streaming in a single-channel and energy-constrained WSN is still very challenging due to three reasons. The first reason is due to the low data rate of the radios used by the energy-constrained sensor nodes, resulting in insufficient bandwidth to support multimedia applications. Multipath load balancing is commonly used in wired networks to increase the aggregated throughput available to an application flow. Applications can take advantage of the multiple paths by splitting the single data stream into multiple sub-streams to be transmitted concurrently via the multiple paths. Multistream video coding techniques like the Multiple Description Coding (MDC) can be used for this purpose. Due to the independent nature of wired links, it is sufficient to use link-disjoint paths [1].

The second reason is due to the broadcast nature of radio propagation in wireless

networks, where nearby sensor nodes interfere with each other's transmissions. This makes the benefits of using multipath load balancing in wireless networks less obvious. When using multiple paths to improve the reliability for data delivery, it is sufficient to use node-disjoint paths, so as to ensure path diversity [1]. However, for effective multipath load balancing in a wireless network, node-disjointedness between paths is necessary but definitely not sufficient. This is due to route coupling that is caused by wireless interferences during simultaneous transmissions along multiple paths within physical proximity of each other. Besides route coupling, wireless interferences from subsequent transmissions along a single multi-hop relay chain of sensor nodes further limit the available bandwidth [2]. Therefore, in order to use multipath load balancing to increase throughputs in a wireless network, a set of physically separated shortest paths (i.e. maximally zone-disjoint shortest paths) that minimize both inter-path and intra-path wireless interferences need to be discovered and used.

The third reason is due to the fact that nodes may interfere beyond their communication ranges and this makes discovering maximally zone-disjoint shortest paths less straightforward. If nodes do not interfere beyond their communication ranges, then the connectivity graph of the network can be used to determine if two nodes interfere with each other. However if nodes interfere beyond their communication ranges, then simply determining the connectivity between the two nodes is not sufficient to determine if they will interfere with each other during concurrent transmissions. The most obvious solution to this problem is to use location information of the two nodes

to determine if they are within interference range of each other. Alternatively, directional antennas can be used to discover a set of maximally zone-disjoint shortest paths. Unfortunately both solutions require special hardware support, making them impractical for the resource-constrained WSN. Therefore it is crucial to consider the effects of both inter-path and intra-path wireless interferences when formulating the multipath load balancing problem, taking into consideration that nodes may interfere beyond their communication ranges.

1.3 Proposed Solutions

In this thesis, three contributions are made. The first contribution is to propose a modeling technique for multipath load balancing. In order to capture the effects of wireless interferences and the physical constraint that nodes may interfere beyond their communication ranges, the use of conflict graphs to model the effects of wireless interferences in a single-channel wireless network is proposed. Conflict graphs are based on the protocol model of interference and have been used previously for this purpose [3]. They indicate which groups of links mutually interfere and hence cannot be active simultaneously. A new metric, the total interference correlation factor for a set of node-disjoint paths, is obtained from the conflict graphs. This metric describes the overall degree of interferences for all the paths in the set, capturing the effects of both inter- and intra-path wireless interferences. It can be used to evaluate the quality of a path-set discovered for multipath load balancing.

The second contribution is to propose a heuristics-based Interference-Minimized Multipath Routing (I2MR) protocol that increases throughputs by discovering and using maximally zone-disjoint shortest paths for load balancing, while requiring minimal localization support and incurring low routing overheads. Localization support is only required at the source node, which is a more powerful sensor node equipped with EO devices and the destination nodes, which are the gateway nodes that link the WSN with the backbone network. Furthermore, directional antennas are not used and the physical constraint that nodes may interfere up to twice their communication ranges is also being considered. The basic idea of I2MR is to mark-out the interference-zone of the first path after it has been discovered and subsequent paths cannot be discovered within this interference-zone. This is analogous to setting up a magnetic field around the first path after it has been discovered. Subsequent paths to be discovered, which are also of the same magnetic charge, naturally maintain a minimum physical separation from the first discovered path due to magnetic repulsion of like charges as shown in Figure 1.3.

The third contribution is to propose a congestion control scheme for I2MR that is able to dynamically adjust the loading-rate of the source, so that the active paths used for load balancing are loaded at the highest possible rate that can be supported, so as to prevent long-term congestions from building-up. This is to increase throughputs further. The basic idea of the scheme is that in the event that intermediate nodes along the active paths detect the on-set of long-term congestions, the source is notified

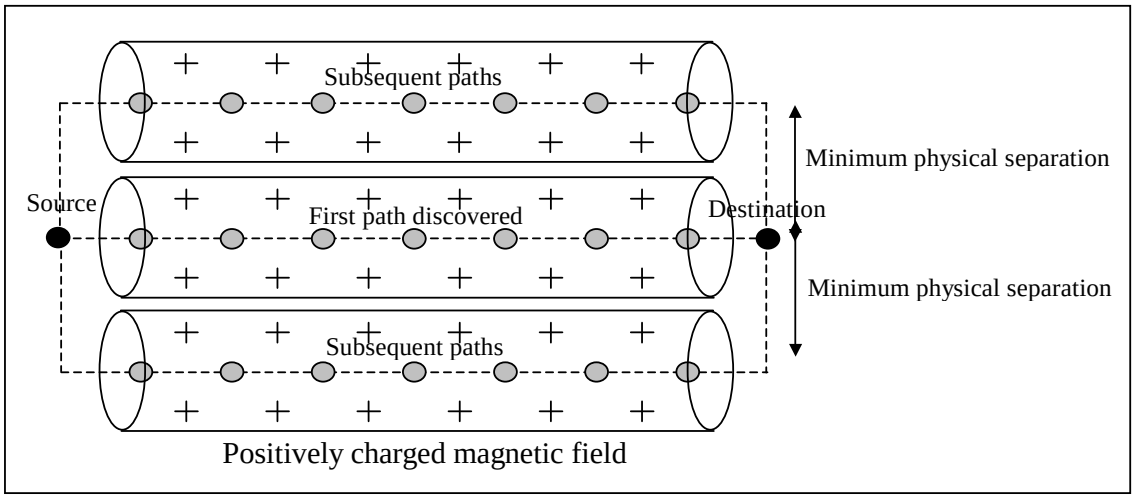

Figure 1.3: Separation between paths due to magnetic repulsion.

to reduce the loading rate to the next lower rate, eventually settling at the highest possible rate supportable by the paths.

Finally, through Global Mobile Information Systems Simulation Library (GloMoSim) simulations, the proposed modeling technique for multipath load balancing is validated. The proposed I2MR protocol and congestion control scheme for I2MR are also evaluated using simulations by comparing the path discovery costs and performances of the path-sets discovered with the unipath Ad-hoc On-demand Distance Vector (AODV) protocol and the multipath Node-Disjoint Multipath Routing (NDMR) protocol. I2MR with congestion control achieves the highest throughputs with up to 260% and 160% gains over AODV and NDMR respectively and the lowest average end-to-end delays. Total energy consumed is also up to 60% lower than NDMR and is comparable or at most 24% more than AODV. High packet delivery ratios are also achieved. Furthermore, the path discovery costs of I2MR is at least comparable or if

not better than NDMR and not prohibitively larger than AODV.

1.4 Thesis Organization

The rest of this thesis is organized as follows: Chapter 2 provides some background information and describes related works on multipath load balancing. Chapter 3 describes the proposed modeling technique for multipath load balancing and provides an illustrative example. Chapter 4 describes the proposed I2MR protocol that discovers maximally zone-disjoint shortest paths used for load balancing. Chapter 5 describes the proposed congestion control scheme for I2MR that dynamically reduces long-term congestions by loading the active paths at the highest possible rate supportable. Chapter 6 describes the GloMoSim simulations used to evaluate and validate the proposed solutions and also presents and discusses simulation results. Chapter 7 concludes this thesis, discusses possible limitations and suggests future works.

Chapter 2

Background and Related Works

Chapter 2 is organized as follow: Sections 2.1 to 2.4 provides relevant background information, while Section 2.5 reviews related works on multipath load balancing. For background information: Section 2.1 reviews routing protocols, Section 2.2 describes video-coding techniques, Section 2.3 presents models for wireless interferences and Section 2.4 describes the network simulator used.

2.1 Routing Protocols

Routing protocols are used to find and maintain routes between source and destination nodes. Two main classes of routing protocols are table-based and on-demand protocols. In table-based protocols [4,5], each node maintains a routing table containing routes to all nodes in the network. Nodes must periodically exchange messages

with routing information to keep routing tables up-to-date. However table-based routing protocols are impractical for the large-scale and energy-constrained WSN. In on-demand protocols [6, 7], nodes only compute routes when they are needed, Therefore, on-demand protocols are more scalable to large-scale networks like WSN. When a node needs a route to another node, it initiates a route discovery process to find a route. The basic route discovery mechanisms of two on-demand routing protocols, AODV and DSR, are briefly described below.

2.1.1 Ad-hoc On-demand Distance Vector (AODV)

AODV [6] uses hop-by-hop routing by maintaining routing table entries at intermediate nodes. The route discovery process is initiated when a source needs a route to a destination and it does not have a route in its routing table. The source floods the network with a route request (RREQ) packet specifying the destination requested. When the destination node receives the RREQ packet, it replies the source with a route reply (RREP) packet along the reverse path. Each node along the reverse path sets up a forward pointer to the node it received the RREP from. This sets up a forward path from the source to the destination. If the node is not the destination, it rebroadcasts the RREQ packet. At intermediate nodes, duplicate RREQ packets are discarded. When the source node receives the first RREP, it begins data transfer to the destination.

2.1.2 Dynamic Source Routing (DSR)

DSR [7] is a source routing protocol, where the source includes the full route in the packet header, which intermediate nodes use to route data packets. The route discovery process is initiated when a source needs a route to a destination and it does not have a route in its routing table. The source floods the network with a RREQ packet specifying the destination requested. The RREQ packet includes a route record, which specifies the sequence of nodes traversed by the packet. When an intermediate node receives a RREQ, it checks to see if it is already in the route record. If it is, it drops the packet, to prevent routing loops. Duplicate RREQs are also dropped. When the destination received the RREQ, it replies with a RREP packet, along the reverse route back to the source. As DSR uses source routing, therefore it does not scale well in large-scale networks like the WSN.

2.2 Video-coding Techniques

The advantage of using multiple paths over single path for video streaming is that it provides a larger aggregate throughput, thus reducing distortion caused by lossy video coders. It also distributes the traffic load in the network more evenly, resulting in shorter network delays. Finally, it provides inherent path diversity that improves reliability. As a result, the receiver can always receive some data during any period, except when all the paths are down simultaneously, which occurs much more rarely

than single path failures. For multipath video streaming to be helpful for streaming compressed video, the video coder has to be properly designed to generate streams so that the loss in one stream does not adversely affect the decoding of the other streams. However, this relative independence between the streams should not be obtained at the great expense in coding efficiency. Therefore, a multi-stream encoder should strive to achieve a good balance. There are two main techniques used: 1) Multiple Descriptions Coding (MDC) [8] and 2) Layered-coding with Selective ARQ (LC-ARQ) [9]. MDC seems to be a more flexible coding technique, as it generates multiple streams that are of equal importance, which means that there need not be any differentiation between the multiple paths used for streaming. The MDC video coding technique is briefly described below.

2.2.1 Multiple Descriptions Coding (MDC)

The MDC [8] is a video coding technique that generates multiple equally important descriptions. The decoder reconstructs the video from any subset of received descriptions, yielding a quality commensurate with the number of received descriptions. In the coder, Multiple Descriptions Motion Compensation (MDMC) is employed. With this coder, two descriptions are generated by sending even pictures as one description and odd pictures as the other, as shown in Figure 2.1. Compared to layered coding like LC-ARQ, MDMC does not require the network or channel coder to provide different levels of protection. Nor does it require any receiver feedback. Acceptable

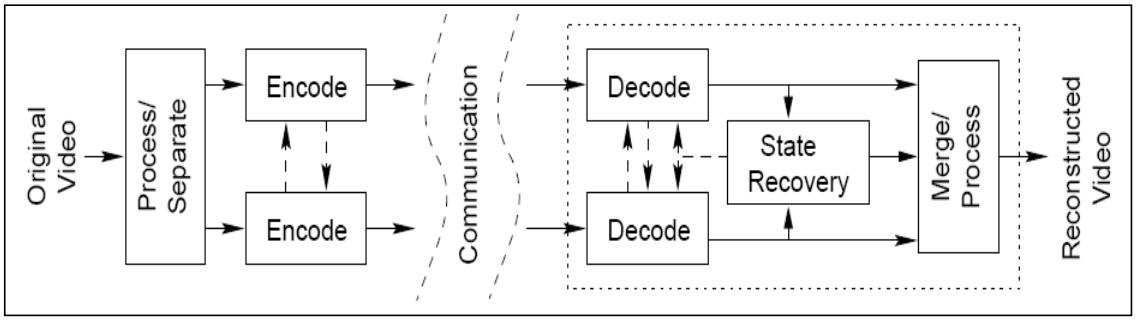

Figure 2.1: Multiple Descriptions Coding (MDC).

quality can be achieved even when both descriptions are subject to relatively frequent packet losses, as long as the losses on the two paths do not occur simultaneously. This strengthens the case of using zone-disjoint multi-paths, as these paths are less correlated and exhibit more independent loss behaviors. Isolated packet losses can be handled more easily using suitable concealment techniques compared to simultaneous burst losses in both paths, which occur less rarely.

2.3 Modeling Wireless Interferences

In order to analyze the problem of multipath load balancing for a single channel wireless network, the effects of wireless interferences need to be factored into the problem formulation. Wireless interferences in a wireless network can be modeled using either by the 1) protocol model of interference or 2) physical model of interference [3]. The protocol model of interference models interference in a binary manner, which means that any signal in the presence of interferences will not be received

correctly at the receiver. It is a simple and useful model that represents the worst-case effects of wireless interferences. However in reality this may not always be the case and the physical model of interference models wireless interferences closer to real-life radios, where the overall Signal-to-Noise Ratio (SNR) at the receiver is used to determine whether a signal can be correctly received in the presence of wireless interferences and ambient noise at the receiver. Due to the simplicity of the protocol model of interference and also that it represents the worst cast effects of wireless interferences, it will be used to model wireless interferences when analyzing the problem of multipath load balancing in a single channel wireless network for this thesis. Both the protocol model of interference and physical model of interference are briefly described below.

2.3.1 Protocol Model of Interference

The protocol model of interference [3] is used to model the worst-case effects of wireless interferences. In this model, a node n_i has a radio with a transmission range of T_i and an interference range $I_i \geq T_i$. The distance between node n_i and n_j is given by d_{ij}. Node n_i can successfully receive a transmission from node n_i if conditions 1 and 2 are satisfied. If physical carrier sensing is used in the Medium Access Control (MAC) protocol, an additional condition 3 is required.

1. $d_{ij} \leq T_i$

2. Any node n_k such that $d_{kj} \leq I_k$ is not transmitting.

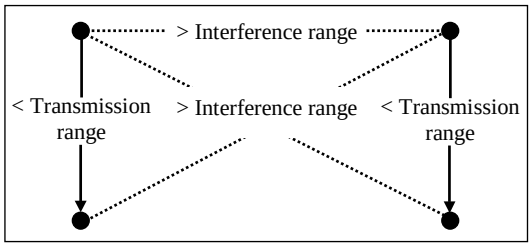

Figure 2.2: Geometric requirements for concurrent transmissions according to the protocol model of interference.

3. Any node n_k such that $d_{ki} \leq I_k$ is not transmitting.

Figure 2.2 illustrates the geometric requirements for concurrent transmissions, If the inequalities are satisfied, both transmissions will succeed, according to the protocol model of interference. The dotted line represents the additional requirement for networks that use physical carrier sensing.

2.3.2 Physical Model of Interference

In the physical model of interference [3], if a node n_i wants to transmit to node n_j, the signal strength $SS_{i,j}$ of n_i's transmission as received at n_j is calculated and the transmission is only successful if and only if $SNR_{i,j} \geq SNR_thresh$, where $SNR_{i,j}$ denotes the SNR at node n_j for the transmissions received from node n_i. The total noise N_j at n_j consists of both the ambient noise N_{amb} and the interference due to other ongoing transmissions in the network. Note that if physical carrier sensing is not used, then there is no requirement that the noise level at the sender must also be low.

2.4 Network Simulator

Protocols for wireless networks are complex to evaluate analytically due to factors such as complex channel access protocols, channel propagation properties and radio characteristics. Excessive execution time of detailed models forms a barrier for the effective use of simulations. The Global Mobile System Simulator (GloMoSim) [10] uses parallel discrete event simulation to reduce execution time for composable detailed simulation model of wireless networks and is briefly described below.

2.4.1 Global Mobile Systems Simulator (GloMoSim)

GloMoSim [10] is a library-based sequential and parallel simulator for wireless networks. It is designed as a set of library modules, each of which simulates a specific wireless communication protocol in the protocol stack. The library has been developed using PARSEC, a C-based parallel simulation language. New protocols and modules can be programmed and added to the library using this language. GloMoSim has been designed to be extensible and composable.

2.5 Review of Related Works

A review of related works shows that, [11] has proposed the deployment of large-scale WSN with high-capacity UAV backbone network support for multimedia streaming, however multipath routing is not used. Much research has been done on multipath

routing for multi-hop and single-channel wireless networks, promising many benefits over unipath routing [1]. Many such works [12–14] discover multiple link- or node-disjoint paths, but use only the best path for data transfer, switching to alternate paths only if the best path fails. This is sufficient to reduce routing overheads and improve reliability, but there may be no performance benefits when using link- or node-disjoint paths for multipath load balancing due to the effects of route coupling and wireless interferences of subsequent nodes along a multi-hop relay chain [2,3,15].

Pearlman et al. [16] demonstrates the benefits of multipath load balancing for multi-channel wireless networks. However they conclude that naively using multiple node-disjoint shortest paths in a single-channel wireless network results in negligible benefits due to severe route coupling. Several works [17, 18] modify the DSR protocol for multipath load balancing, naively using multiple node-disjoint shortest paths. Their results show slight improvements in performance over unipath routing, suggesting the possibility of an interference-aware multipath routing protocol to achieve better performances.

Wu and Harms [19] define the correlation factor of two node-disjoint paths as the number of links connecting the two paths and use it as a path-selection metric to select the pair of least-correlated paths for multipath load balancing. However, they assume nodes do not interfere beyond their communication range, which typically is not the case as shown in [20].

Jain et al. [3] considers the effects of wireless interferences by using a graph-based

analytical model to compute the upper and lower bounds on the optimal throughput for a given network and workload. While their method is able to discover interference-minimized paths without assuming interference range to be at most communication range, it is computationally too intensive to be practical for large-scale and resource-constrained WSN.

Nguyen et al. [21] draws inspiration from electric field lines to select physically separated paths for multipath load balancing. Unfortunately, special localization hardware is required for each node, making it impractical for resource-constrained WSN. Similarly, other proposals [22, 23] that use directional antennas to discovery zone-disjoint paths are also not feasible for resource-constrained WSN.

A novel idea to discover zone-disjoint paths, without requiring special hardware support or assuming that interference range is at most communication range, is proposed in [2]. Interference correlation is computed by estimating the distance between two nodes to be the shortest path hop count multiplied by communication range. Unfortunately, each node requires the complete network topology, which is only possible with a link-state routing protocol. It is well known that a link-state routing protocol scales poorly for large-scale networks due to prohibitive memory and computation requirements. Therefore this technique is also not suitable for large-scale resource-constrained WSN.

Based on related works reviewed in this section, there does not seem to exist a prctical multipath discovery technique that efficiently discovers zone-disjoint paths

for multipath load balancing in large-scale, resource-constrained and single-channel WSN, without requiring special hardware on every node or assuming that interference range is at most communication range.

Chapter 3

Modeling Multipath Load Balancing

Chapter 3 is organized as follow: Section 3.1 reviews the use of graph theory to model a general communications network. Section 3.2 describes the technique used for modeling multipath load balancing in a wired network. For Section 3.3: Sections 3.3.1 and 3.3.2 describe the technique used for modeling multipath routing in a wireless network, Section 3.3.3 presents the proposed technique used to evaluate the quality of a path-set discovered for multipath load balancing in a wireless network and Section 3.3.4 provides an example as illustration.

3.1 General Communications Network

Consider a static network with N nodes arbitrarily located on a plane of area A. Let n_i, where $1 \leq i \leq N$, denotes the nodes and $d_{ij} = D(n_i, n_j)$ denotes the distance between nodes n_i and n_j. The network can be modeled using a connectivity graph $G(V, E)$, where V is the set of N nodes and E is the set of directed links connecting nodes in V. A directed link from n_i to n_j, where $n_i, n_j \in V$, is represented by $l_{i,j} = L(n_i, n_j)$. The actual link bandwidth (i.e. raw data rate of link) and the available link bandwidth (i.e. link bandwidth available for an application flow) of link $l_{i,j} \in E$ are represented by $b_{i,j}^{actual} = B^{actual}(l_{i,j}) > 0$ and $b_{i,j} = B(l_{i,j}) > 0$ respectively. Due to protocol overheads and cross traffic of other application flows, therefore $b_{i,j} < b_{i,j}^{actual}$.

3.2 Wired Network

Consider the communication between a single source s and single destination d. A path p from source node $n_s \in V$ to destination node $n_d \in V$ is represented by the node set, $P_p^{s,d} = \{n_s, n_d\} \cup IP_p^{s,d}$ that comprises of nodes n_s, n_d and a sequence of $K_{p=p}$ intermediate nodes n_p^k between n_s and n_d without loops, represented by the set $IP_p^{s,d} = \{n_p^k\} \in V$, $\forall k$ where $1 \leq k \leq K_{p=p}$. Let n_p^k represents the k^{th} intermediate node along the path p. The number of nodes along path p is represented by $|P_p^{s,d}| = |IP_p^{s,d}| + 2 = K_{p=p} + 2$.

Alternatively, a path p from n_s to n_d, can also be represented by the link set, $P_p^{'s,d} = \{l_p^{s,1}, l_p^{K_{p=p},d}\} \cup IP_p^{'s,d}$ that comprises of directed links $l_p^{s,1}$, $l_p^{K_{p=p},d}$ and a sequence of directed links $l_p^{k,(k+1)}$ between two adjacent intermediate nodes n_p^k and $n_p^{(k+1)}$ between n_s and n_d without loops, represented by the set $IP_p^{'s,d} = \{l_p^{k,(k+1)}\} \in E$, $\forall k$ where $1 \leq k \leq (K_{p=p} - 1)$. Let $l_p^{k,(k+1)}$ represents the directed link from n_p^k to $n_p^{(k+1)}$ along the path p. The length or total number of hops (links) of path p is represented by $|P_p^{'s,d}| = |IP_p^{'s,d}| + 2 = (K_{p=p} - 1) + 2 = K_{p=p} + 1$, where $K_{p=p}$ is the total number of intermediate nodes along the path.

Let $MP^{s,d}$ define the set of all possible P paths from n_s to n_d, such that $MP^{s,d} = \{P_p^{s,d}\}$, $\forall p$ where $1 \leq p \leq P$. Alternatively, the set of all possible paths from n_s to n_d can also be represented by $MP^{'s,d} = \{P_p^{'s,d}\}$, $\forall p$ where $1 \leq p \leq P$. For single-path routing, $|MP^{s,d}| = |MP^{'s,d}| = P = 1$. For multipath routing, $2 \leq (|MP^{s,d}| = |MP^{'s,d}|) \leq P$.

In a static wired network where the links are independent of each other and are not affected by wireless interferences, simultaneous transmissions of nearby links do not interfere with each other. Therefore for single-path routing, where $|MP^{s,d}| = |MP^{'s,d}| = P = 1$, let $B(P_1^{'s,d}) > 0$ represents the available bandwidth of the single routing path $P_1^{'s,d} \in MP^{'s,d}$ from n_s to n_d for an application flow. Since all the links are independent, therefore $B(P_1^{'s,d}) = min\{B(l_1^{k,(k+1)})\} = min\{b_1^{k,(k+1)}$, $\forall k$ where $1 \leq k \leq (K_{p=1} - 1)$. In other words, the available bandwidth of the single routing path for an application flow is the bottleneck bandwidth of the links along the path.

For multipath routing, where $2 \leq (|MP^{s,d}| = |MP'^{s,d}|) \leq P$, let $B(P'^{s,d}_p) > 0$, for $1 \leq p \leq P$, represents the available bandwidth or throughput of a routing path $P'^{s,d}_p \in MP'^{s,d}$ from n_s to n_d for an application flow. For multipath load balancing using P link-disjoint routing paths, $P'^{s,d}_{p1} \cap P'^{s,d}_{p2} = \oslash$, $\forall P'^{s,d}_{p1}, P'^{s,d}_{p2} \in MP'^{s,d}$ where $1 \leq (p1, p2) \leq P$ and $p1 \neq p2$. Let $B(MP'^{s,d})$ represents the overall aggregated bandwidth of the set of P paths from n_s to n_d available for an application flow. Since all the links are independent, implies that the P paths are also independent. Therefore $B(MP'^{s,d}) = \sum_{\forall p, 1 \leq p \leq P} B(P'^{s,d}_p)$. In other words, the aggregated bandwidth of the P paths from n_s to n_d available for an application flow is the sum of all the available bandwidth of each of the paths. Since $B(P'^{s,d}_p) > 0$, implies that $\sum_{\forall p, 1 \leq p \leq (P+1)} B(P'^{s,d}_p) > \sum_{\forall p, 1 \leq p \leq P} B(P'^{s,d}_p)$. Therefore for wired networks, using an additional link-disjoint path for load balancing will always result in an increase in the overall aggregated bandwidth available for an application flow from n_s to n_d. This property may not hold true for wireless networks due to route coupling.

3.3 Wireless Network

Multipath load balancing in a single-channel wireless network is not as straightforward as in a wired network. This is due to the broadcast nature of radio propagation resulting in wireless interferences between nearby wireless links. Therefore the links are no longer independent of each other, which implies that the set of node-disjoint

paths used for load balancing may be coupled. Due to the effects of wireless interferences and route coupling, the overall bandwidth available for an application flow between n_s and n_d using multipath load balancing in a wireless network will be smaller than that for a wired network, using the same number of paths.

In order to analyze the problem of multipath load balancing for a single-channel wireless network, the effects of wireless interferences need to be factored into the problem formulation. Wireless interferences in a wireless network can be modeled using either the protocol model of interference or the physical model of interference as described in Section 2.3. Due to the simplicity of the protocol model of interference and also that it represents the worst-case effects of wireless interferences, it will be used to model wireless interferences when analyzing the problem of multipath load balancing in a single-channel wireless network.

To simplify the analysis, assume that all the nodes in the wireless network have a uniform transmission range of T and a potentially larger interference range of $T \leq I \leq 2T$. Considering the worst-case scenario, let $I = 2T$. Assume that no physical carrier sensing is used. The static single-channel wireless network can then be modeled using a connectivity graph $G = (V, E)$, where V is the set of nodes in the network and E is the set of directed wireless links between the nodes in V. There is a directed link $l_{i,j} = L(n_i, n_j) \in E$, from node $n_i \in V$ to node $n_j \in V$, where $i \neq j$, if the condition $d_{i,j} \leq T_i$ is satisfied.

3.3.1 Correlation Factor Metric

The correlation factor metric can be used to describe the degree of wireless interferences between two node-disjoint paths [19]. The correlation factor (η) of two node-disjoint paths is defined as the number of links connecting the two paths, which can be easily inferred from the connectivity graph (G) of the network. If there is no link ($\eta = 0$) between the two node-disjoint paths, then the two paths are unrelated. Otherwise, the two paths are η-related. The total correlation factor of a set of multiple paths is defined as the sum of the correlation factor of each pair of paths, which can be used to evaluate the quality of a path-set used for wireless multipath load balancing.

The main limitation of using the connectivity graph (G) of the network to derive the correlation factor metric (η) is that the additional physical constraint that nodes may interfere beyond their communication ranges (i.e. $T \leq I \leq 2T$) cannot be captured in the problem formulation. For simplicity, the worst-case scenario where $I = 2T$ is considered in the analysis. Another limitation is that the correlation factor metric (η) only captures the effects of inter-path interferences between two node-disjoint paths, but it is not able to capture the effects of intra-path interferences along the individual paths.

3.3.2 Conflict Graph

In order to incorporate the added constraint that $I = 2T$ into the problem formulation, a conflict graph $H = (E, C)$ is constructed, whose vertices correspond to the links in the connectivity graph, G [3]. There is an edge between vertices $l_{i,j}$ and $l_{p,q}$ in H if $l_{i,j}$ and $l_{p,q}$ may not be active simultaneously (i.e., mutually interfering links). The edges in C represent all the possible interferences between the links in E. Based on the protocol model of interference, an edge is drawn from vertex $l_{i,j}$ to $l_{p,q}$ in H if $d_{i,q} \leq I_i$, and from vertex $l_{p,q}$ to $l_{i,j}$ in H if $d_{p,j} \leq I_p$. This encompasses the case where a conflict arises because links $l_{i,j}$ and $l_{p,q}$ have a node in common (i.e., $i = p$ or $i = q$ or $j = p$ or $j = q$). Additional conditions are required if physical carrier sensing is used. Note that an edge is not drawn from a vertex to itself in the conflict graph, H.

3.3.3 Proposed Technique

First consider a single application flow between n_s and n_d, ignoring the effects of cross traffic or background traffic. Based on the conflict graph (H) obtained from the static single-channel wireless network, the following definitions are made:

Definition 1. **Link interference correlation factor, $\eta_{i,j}$,** of $l_{i,j} \in E$ is defined as the number of outgoing edges from the vertex $l_{i,j}$ in the conflict graph, H, $\forall i, j$ where $1 \leq (i, j) \leq N$.

Definition 2. **Path interference correlation factor, $\eta_p^{'}$,** of $P_p^{'s,d} \in MP^{'s,d}$ is

defined as $\eta_p^{'} = \eta_{l,s} + \sum_{\forall k, 1 \leq k \leq (K_{p=p}-1)} \eta_{k,(k+1)} + \eta_{(K_{p=p}-1),d}$, where $K_{p=p} = |IP_p^{s,d}|$, $\forall p$ where $1 \leq p \leq P$.

Definition 3. **Total interference correlation factor,** $\eta_{total(P)}$**,** of $MP'^{s,d}$ is defined as $\eta_{total(P)}^{'}(t_0) = \sum_{\forall p, 1 \leq p \leq P} \eta_p^{'}$, where $MP'^{s,d} = \{P_p'^{s,d}\}$, $\forall p$ where $1 \leq p \leq P$. This metric can be used to evaluate the path-set used for wireless multipath load balancing between n_s and n_d. Furthermore, it captures both the added constraint that $I = 2T$ and also the effects of intra-path interferences along the individual paths in the path-set. A path-set with a smaller total interference correlation factor is expected to perform better (i.e. higher aggregated throughput) when used for multipath load balancing than a path-set with a larger total interference correlation factor.

Definition 4. **Minimum path interference correlation factor,** $\eta_{p\,min}^{'}$**,** of $P_p^{s,d} \in MP^{s,d}$ is defined as $\eta_{p\,min}^{'} = (3(K_{p=p} - 1) - 1) + 3 = 3K_{p=p} - 1$, where $K_{p=p} = |IP_p^{s,d}|$ and $I = 2T$.

In single path routing, where $|MP^{s,d}| = |MP'^{s,d}| = P = 1$, the path interference correlation factor, $\eta_1^{'}$, of $P_1^{s,d} \in MP^{s,d}$ is minimized when $d_{s,1} = d_{K_{p=1},d} = d_{k,(k+1)} = T$, $\forall n_1^k \in IP_1^{s,d}$ where $1 \leq k \leq (K_{p=1} - 1)$, represented by $\eta_{1\,min}^{'}$. One possible configuration of $n_1^k \in IP_1^{s,d}$ that will achieve $\eta_{1\,min}^{'}$ is when n_1^k lie on a straight line joining n_s and n_d, $\forall k$ where $1 \leq k \leq K_{p=1}$. This interference-minimized single-hop routing path can be achieved using the shortest-hop routing path between n_s and n_d. If the available bandwidth, $b_{k,(k-1)}$, of $l_1^{s,1}$, $l_1^{K_{p=1},d}$ and $l_1^{k,(k+1)} \in IP_1^{'s,d}$, $\forall k$ where $1 \leq$

$k \leq (K_{p=1}-1)$, is constant (i.e. $b_{k,(k-1)} = b$), then the bandwidth of the single routing path, $P_1^{s,d}$, available for an application flow is given by $B(P_1^{'s,d}) = \frac{1}{4}(b_{k,(k-1)}) = \frac{b}{4}$, $\forall k$ where $1 \leq k \leq (K_{p=1} - 1)$.

In multipath routing, the objective is to discover a set, $MP^{'s,d}$, of P paths that minimizes the overall interference correlation factor, $\eta^{'}_{total(P)}$, of $MP^{'s,d}$, so that the P paths can be used concurrently for effective load balancing between n_s and n_d. Starting with $p = 1$ and $MP^{'s,d} = \oslash$, the first routing path, $P_1^{s,d}$, discovered that minimizes $\eta^{'}_{total(1)}$ (i.e. $\eta^{'}_{total(1)} \rightarrow \eta^{'}_{total(1)\,min} = \eta^{'}_{1\,min}$) and $|P_1^{s,d}|$ will be the shortest-hop routing path between n_s and n_d. Path $P_1^{s,d}$ is then added to $MP^{'s,d}$ (i.e. $MP^{'}_{s,d} = P_1^{s,d} \cup \oslash$). The second routing path, $P_2^{s,d}$, that is discovered, attempts to minimize $\eta^{'}_{total(2)}$ (i.e. $\eta^{'}_{total(2)} \rightarrow \eta^{'}_{total(2)\,min} = \eta^{'}_{1\,min} + \eta^{'}_{2\,min}$) and $|P_2^{s,d}|$, such that $P_1^{s,d}$ and $P_2^{s,d}$ are sufficiently separated physically so that there is minimal route coupling between them and the length of $P_2^{s,d}$ is the shortest possible. Path $P_2^{s,d}$ is subsequently added to $MP^{'s,d}$ (i.e. $MP^{'s,d} = P_2^{s,d} \cup \{P_1^{s,d}\}$). Similarly the k^{th} routing path, $P_k^{s,d}$, that is discovered similarly attempts to minimize $\eta^{'}_{total(k)}$ (i.e. $\eta^{'}_{total(k)} \rightarrow \eta^{'}_{total(k)\,min} = \sum_{\forall q, 1 \leq q \leq k} \eta^{'}_{q\,min}$) and $|P_k^{s,d}|$. Path $P_k^{s,d}$ is subsequently added to $MP^{'s,d}$ (i.e. $MP^{'}_{sd} = P_k^{sd} \cup \{P_p^{sd}\}$, $\forall p$ where $1 \leq p \leq (k-1)$). This route discovery process is repeated until all the P maximally zone-disjoint paths have been discovered and added to path set $MP^{'s,d}$, such that $|MP^{'s,d}| = P$.

The main purpose of discovering the set, $MP^{'s,d}$, that comprises of P maximally zone-disjoint paths where route coupling is minimal between the paths, is to maximize

the overall aggregated bandwidth available for an application flow between n_s and n_d. Ideally if there is no route coupling between all the P paths in $MP'^{s,d}$, then the overall aggregated bandwidth of the P paths from n_s to n_d available for an application flow, $B(MP'^{s,d})$, is the sum of all the available bandwidth of the individual routing paths in $MP'^{s,d}$ (i.e. $B(MP'^{s,d}) = \sum_{\forall p, 1 \leq p \leq P} B(P_p'^{s,d})$), which is similar to that of a wired network. Therefore, the maximum overall aggregated bandwidth of the P paths used for load balancing, available for an application flow between n_s and n_d, is given by $B_{max}(MP'^{s,d}) = \sum_{\forall p, 1 \leq p \leq P} B(P_p'^{s,d}) = P(\frac{b}{4})$.

Therefore, the multipath load balancing problem in a single-channel static wireless network can be formally formulated as: To efficiently discover, with minimum route discovery overheads, a set, $MP'^{s,d}$, that comprises of P maximally zone-disjoint shortest paths that minimize $\eta'_{total(p)}$ and $|P_p^{s,d}|$, $\forall p$ where $1 \leq p \leq P$, so that the overall aggregated bandwidth available for an application flow between n_s and n_d, is maximized (i.e. $B(MP'^{s,d}) \rightarrow B_{max}(MP'^{s,d}) = P(\frac{b}{4})$). The next section provides an example to illustrate the proposed technique.

3.3.4 Illustrative Example

The assumptions made of the network are as follows:

1. Wireless static network.

2. Single radio and channel for all nodes.

3. Uniform transmission range T and interference range I for all nodes.

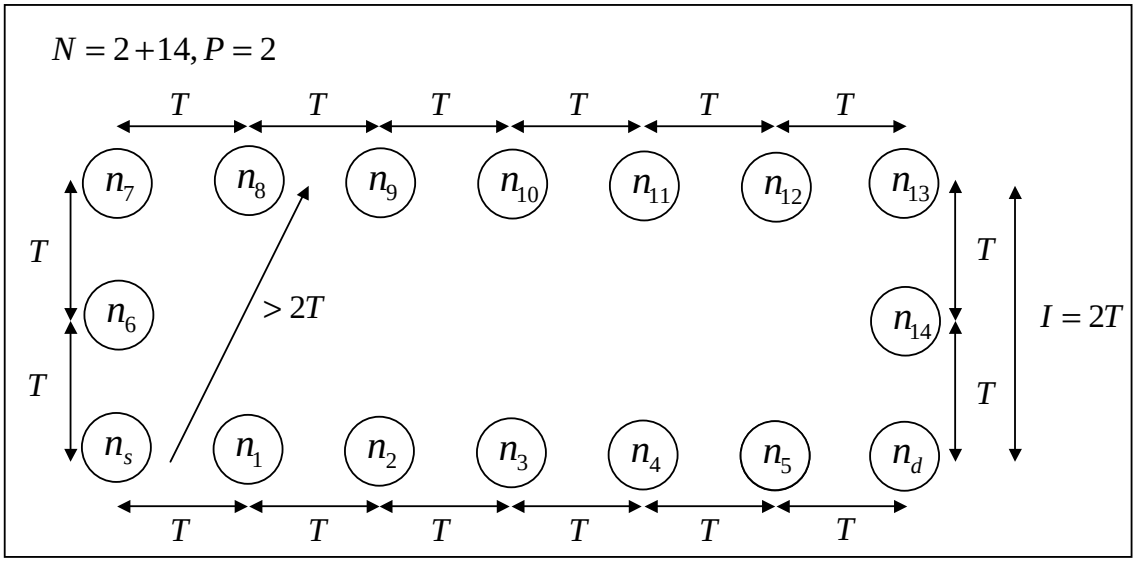

Figure 3.1: Network topology.

4. Interference range is twice transmission range $I = 2T$.

5. Single source node n_s and single destination node n_d.

6. Single application flow from n_s to n_d.

7. No cross traffic and background traffic.

8. Uniform available bandwidth (b) for all links.

The network topology of a network comprising of 1 source, 1 destination and 14 intermediate nodes is as shown in Figure 3.1. The connectivity graph $G = (V, E)$ of the network in Figure 3.1 is as shown in Figure 3.2 and only forward links are considered. From the connectivity graph G, the following are obtained:

1. Node set of path 1, $P_1^{s,d} = \{n_s, n_d\} \cup IP_1^{s,d}$, where

   $IP_1^{s,d} = \{n_1^1, n_1^2, n_1^3, n_1^4, n_1^5\}$ and $|IP_1^{s,d}| = 5$.

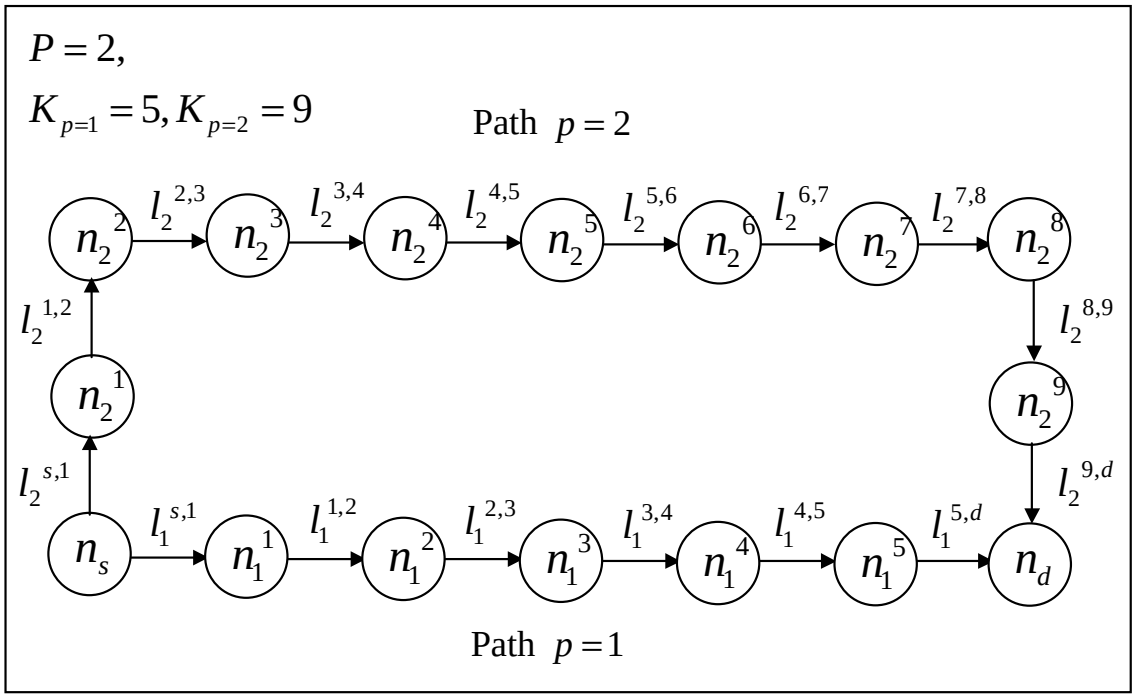

Figure 3.2: Connectivity graph $G = (V, E)$ of network.

2. Node set of path 2, $P_2^{s,d} = \{n_s, n_d\} \cup IP_2^{s,d}$, where

   $IP_2^{s,d} = \{n_2^1, n_2^2, n_2^3, n_2^4, n_2^5, n_2^6, n_2^7, n_2^8, n_2^9\}$ and $|IP_2^{s,d}| = 9$.

3. Link set of path 1, $P_1^{'s,d} = \{l_1^{s,1}, l_1^{K_{p=1},d}\} \cup IP_1^{'s,d}$, where

   $IP_1^{'s,d} = \{l_1^{1,2}, l_1^{2,3}, l_1^{3,4}, 1_1^{4,5}\}$ and $|IP_1^{'s,d}| = 4$.

4. Link set of path 2, $P_2^{'s,d} = \{l_2^{s,1}, l_2^{K_{p=2},d}\} \cup IP_2^{'s,d}$, where

   $IP_2^{'s,d} = \{l_2^{1,2}, l_2^{2,3}, l_2^{3,4}, 1_2^{4,5}, 1_2^{5,6}, 1_2^{6,7}, 1_2^{7,8}, 1_2^{8,9}\}$ and $|IP_2^{'s,d}| = 8$.

5. Set of $P = 2$ paths from n_s to n_d, $MP^{s,d} = \{P_1^{s,d}, P_2^{s,d}\}$.

6. Size of path-set, $|MP^{s,d}| = 2$.

7. Total number of nodes, $N = |V| = |IP_1^{s,d}| + |IP_2^{s,d}| + 2 = 16$.

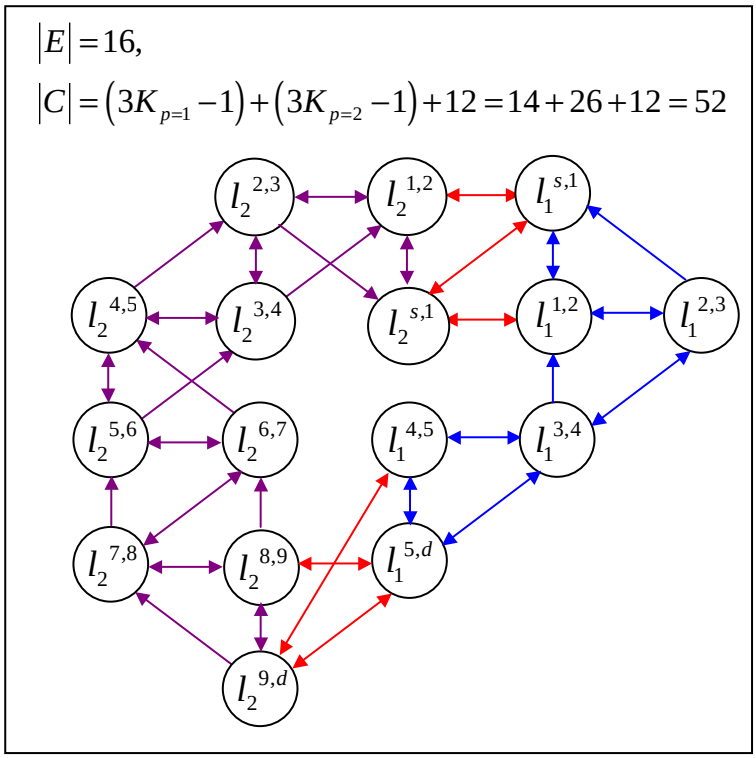

Figure 3.3: Conflict graph $H = (E, C)$ of network.

8. Total number of links, $|E| = |IP_1^{'s,d}| + |IP_2^{'s,d}| + 2P = 16$.

The conflict graph $H = (E, C)$ of the network in Figure 3.1 is as shown in Figure 3.3. From the conflict graph H, the following are obtained:

1. Link interference correlation factors for links along path 1 are

   $\eta_1^{s,1} = \eta_1^{1,2} = \eta_1^{2,3} = \eta_1^{4,5} = 3$ and $\eta_1^{3,4} = \eta_1^{5,d} = 4$.

2. Link interference correlation factors for links along path 2 are

   $\eta_2^{s,1} = \eta_2^{1,2} = \eta_2^{2,3} = \eta_2^{3,4} = \eta_2^{4,5} = \eta_2^{5,6} = \eta_2^{6,7} = \eta_2^{7,8} = 3$ and $\eta_2^{8,9} = \eta_2^{9,d} = 4$.

3. Path interference correlation factor for path 1,

   $\eta_1^{'} = \eta_1^{s,1} + \sum_{\forall k, 1 \leq k \leq 4} \eta_1^{k(k+1)} + \eta_1^{s,d} = \eta_1^{s,1} + \eta_1^{1,2} + \eta_1^{2,3} + \eta_1^{3,4} + \eta_1^{4,5} + \eta_1^{5,d}$

$= 20 > \eta^{'}_{1\,min} = 3K_{p=1} - 1 = 14$

4. Path interference correlation factor for path 2,

   $\eta^{'}_2 = \eta^{s,1}_2 + \sum_{\forall k, 1 \leq k \leq 8} \eta^{k(k+1)}_2 + \eta^{9,d}_2$

   $= \eta^{s,1}_2 + \eta^{1,2}_2 + \eta^{2,3}_2 + \eta^{3,4}_2 + \eta^{4,5}_2 + \eta^{5,6}_2 + \eta^{6,7}_2 + \eta^{7,8}_2 + \eta^{8,9}_2 + \eta^{9,d}_2$

   $= 32 > \eta^{'}_{2\,min} = 3K_{p=2} - 1 = 26$

5. Total interference correlation factor for path-set,

   $\eta^{'}_{total(2)} = \sum_{\forall p, 1 \leq p \leq 2} \eta^{'}_p = \eta^{'}_1 + \eta^{'}_2 = 20 + 32 = 52$

   $> \eta^{'}_{total(2)\,min} = \sum \forall p, 1 \leq p \leq 2 \eta^{'}_{p\,min} = \eta^{'}_{1\,min} + \eta^{'}_{2\,min} = 14 + 26 = 40.$

   Since, $\eta_{total(2)'} > \eta_{total(2\,min)'}$

   $\Rightarrow$ route coupling for path-set.

6. Overall aggregated available bandwidth for path-set,

   $B(MP^{'}_{s,d}) < B_{max}(MP^{'}_{s,d}) = \sum_{\forall p, 1 \leq p \leq 2} B_{max}(P^{'s,d}_p) = 2(\frac{b}{4}) = (\frac{b}{2}).$

Chapter 4

Interference-Minimized Multipath Routing (I2MR) Protocol

Chapter 4 is organized as follow: Section 4.1 defines the problem and gives a brief overview of the proposed I2MR protocol. Section 4.2 provides details of the three basic steps of I2MR path discovery: 1) Primary path discovery in Section 4.2.1, 2) Interference-zone marking in Section 4.2.2 and 3) Secondary and backup path discovery in Section 4.2.3.

4.1 Problem Definition and Overview

Section 4.1.1 first defines the problem and states the assumptions made before Section 4.1.2 gives a brief overview of the proposed I2MR protocol.

4.1.1 Problem Definition

The main focus of this thesis is on the efficient multi-hop relay of time-sensitive target information that is continuously captured by the sensor with EO via the single-channel and energy-constrained WSN to the nearest gateway nodes linking to the UAV backbone network. The problem is being defined as a multipath and multi-hop routing problem, where the source is the sensor with EO and the final destination is the backbone node connecting directly to the gateway nodes. The source attempts to construct up to three zone-disjoint paths, (i.e. primary, secondary and backup paths) to the final destination as shown in Figure 4.1. The gateway nodes along these paths will be known as the primary, secondary and backup destinations respectively. The source uses both primary and secondary paths concurrently for load balancing and switches to the backup path only when either path fails, thus minimizing path rediscovery overheads. The rationale of using two paths for load balancing is that there is little or no gain in aggregate throughput from using more than two paths [2].

The following assumptions are made:

1. Ground WSN nodes are all static (i.e. non-mobile).

2. Interference range is at most twice communication range.

3. Location of source and gateway nodes are known.

4. Multiple gateway nodes connect directly to a backbone node using high capacity and non-interfering data links.

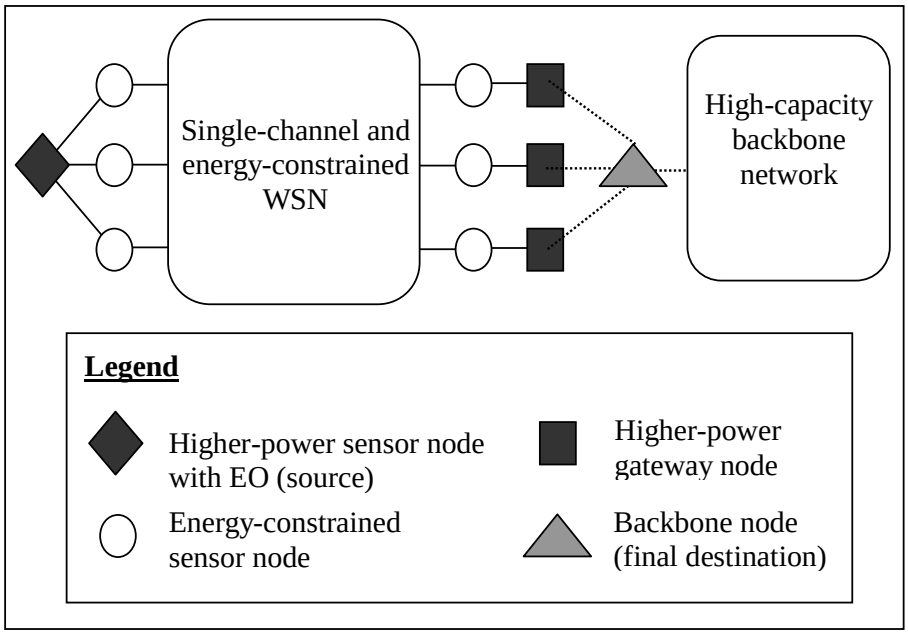

Figure 4.1: Zone-disjoint paths from source to final destination.

5. Source and gateway nodes are much less energy-constrained.

6. Souce-final destination pairs suitably spaced out.

7. Received signal strength indication (RSSI) is available for estimating relative distance.

8. MAC layer operates in promiscuous mode.

4.1.2 Protocol Overview

The source initiates I2MR path discovery to the final destination. The three basic steps of I2MR path discovery are:

1. *Primary path discovery*: Constructs shortest possible path from source to primary destination that minimizes intra-path interference.

2. *Interference-zone marking*: Marks one- and two-hop neighbors of intermediate nodes of primary path as interference-zone of primary path with low overheads. Up to two-hop neighbors are marked because interference range is assumed to be at most twice communication range.

3. *Secondary and backup path discovery*: Selects secondary and backup destinations and constructs shortest paths back to the source. Paths constructed are outside the interference-zone of the primary path and minimize intra-path interference.

After successful path-discovery, the source uses the primary-secondary path-pair concurrently for load balancing, keeping the third path as the backup path.

4.2 Protocol Details

The next three sections provide further details on the three basic steps of the I2MR path discovery.

4.2.1 Primary Path Discovery

The objective is to construct the shortest path from source to primary destination that minimizes intra-path interference. We modify the path discovery of AODV,

```
1   /*d_ij: estimated distance between node i and node j*/
2   /*delay: random delay for RREQ broadcast*/
3   /*D_comm: communication range of node*/
4   if (d_ij ≥ 0.7 * D_comm) { /*further than min. distance required*/
5      delay = ComputeBcastDelay(d_ij); /*see line 11*/
6      BroadcastRREQ(delay);
7   } else
8      DropRREQ( );
9
10  /*function that computes the random broadcast delay*/
11  ComputeBcastDelay(d_ij) {
12     /*the larger the d_ij, the smaller the offset*/
13     delay = offset + random(0,1) * BCAST_JITTER;
14     return delay;
15  }
```

Figure 4.2: Broadcast RREQ algorithm. Invoked when intermediate node i receives RREQ from node j.

where the source searches a route by flooding a RREQ packet. We choose to modify the path discovery of AODV because on-demand protocols are more suitable than table-based protocols and AODV is more scalable than DSR for large-scale WSN. An intermediate node after processing a non-duplicate RREQ, utilizes the algorithm in Figure 4.2 to broadcast the RREQ packet. Ensuring minimum spacing between neighboring nodes along a path minimizes intra-path interference and by allowing only the primary destination reply with RREP to the first RREQ it receives ensures the shortest path discovered. Route caching is not used. Simulation results show that the paths discovered are not significantly longer than those discovered without the modifications.

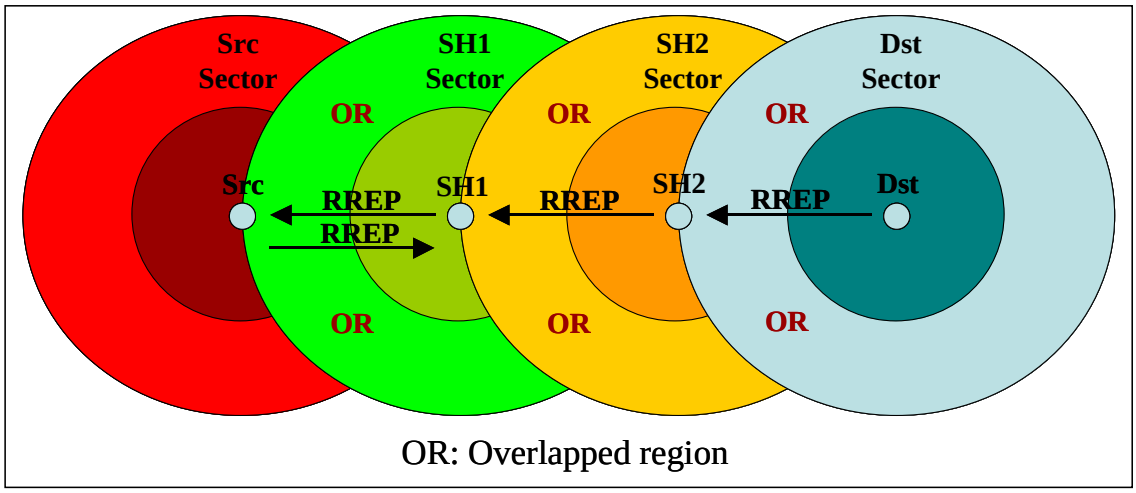

Figure 4.3: Marking sectors and overlapped regions.

4.2.2 Interference-Zone Marking

The objective is to mark the interference-zone of the primary path with minimum control bytes transmitted (i.e. low overheads), so that nodes marked as within the interference-zone of the primary path do not participate in the path discoveries for both secondary and backup paths. Interference-zone marking involves three simple steps:

1. *Sector marking*: Assigns nodes along primary path as Sector Heads (SH) and classify their neighbors into their respective sectors. Overlapped regions of adjacent sectors are also identified. Sector marking is done during the RREP phase of primary path discovery and is as shown in Figure 4.3. Non-SH nodes overhearing RREP from SHs utilize the algorithm in Figure 4.4 to assign their respective sectors.

2. *Broadcast Zone-marker Potential (BZP) assignment*: Assigns different BZPs for

```
1  /*addrOwnSH_i: sector head address of node i*/
2  /*fOLapped_i: mark overlapped region flag of node i*/
3  if (addrOwnSH_i = NULL){ /*own sector not assigned*/
4     addrOwnSH_i = SHj; /*assign to sector j*/
5  } else {
6     if (addrOwnSH_i! = SHj) /*SH j not own SH*/
7        fOLapped_i = TRUE; /*mark as overlapped region*/
8  }
```

Figure 4.4: Sector assignment algorithm. Invoked when non-SH node i overhears RREP from SH j.

different regions of each sector. Nodes that are not in the overlapped regions and furthest away from their respective SHs are assigned higher BZPs as shown in Figure 4.5. Figure 4.6 lists the possible BZP assignments in decreasing priorities. BZP assignment is initiated by the source sending a RMARK packet along the primary path to the primary destination. A SH upon receiving the RMARK packet, immediately broadcasts the MARK_IZ1 (MIZ1) packet to assign BZPs. Non-SH nodes upon overhearing MIZ1 from their own SHs, utilize the algorithm in Figure 4.7 to assign their respective BZPs.

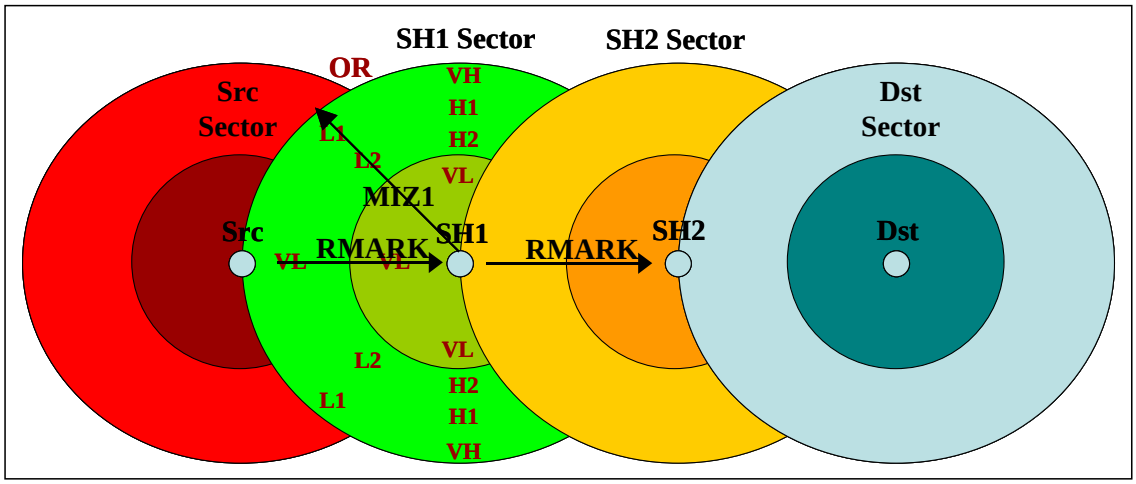

Figure 4.5: Assigning different BZPs for different regions of a sector.

1	*VERY_HIGH*	*VH*
2	*HIGH_LV1*	*H1*
3	*HIGH_LV2*	*H2*
4	*LOW_LV1*	*L1*
5	*LOW_LV2*	*L2*
6	*VERY_LOW*	*VL*

Figure 4.6: BZP assignments in decreasing priorities.

3. *Zone marking*: Marks one- and two-hops neighbors of SHs as either Interference-Zone1 (IZ1) or Interference-Zone2 (IZ2). A SH upon receiving RMARK, broadcasts the MIZ1 packet. Non-SH nodes overhearing MIZ1 invoke the algorithm shown in Figure 4.8. Nodes assigned higher BZPs have higher probability to broadcast the MARK_IZ2 (MIZ2) packet. Non-SH nodes overhearing MIZ2 broadcasts from one-hop neighbors invoke the algorithm as shown in Figure 4.9. The Downgrade Policy attempts to distribute MIZ2 broadcasts evenly within each sector. A node will not broadcast MIZ2 if the number of MIZ2 overheard in its own sector exceeds a pre-defined limit. Furthermore, if the number of MIZ2 overheard by a SH in its own sector exceeds a pre-defined limit, SH immediately relays RMARK downstream, which will prevent further MIZ2 broadcasts within the sector. This ensures that minimal MIZ2 broadcasts by one-hop neighbors are required for effective marking of IZ2.

4.2.3 Secondary and Backup Path Discovery

The objective is to construct the shortest secondary and backup paths from the secondary and backup destinations respectively back to the source that minimize

```
1   /*d_ij: estimated distance between node i and SH j*/
2   /*fOLapped_i: mark overlapped region flag of node i*/
3   /*bzp_i: broadcast zone-marker potential marking of node i*/
4   /*D_comm: communication range of node*/
5   if (d_ij ≤ 0.7 * D_comm) { /*within VERY_LOW BZP band*/
6     bzp_i = VL; /*mark BZP as VERY_LOW*/
7   } else {
8     if (fOLapped_i) { /*marked as overlapped region*/
9       if (d_ij − 0.7 * D_comm ≥ 0.3 * D_comm/2) /*more than half comms range*/
10        bzp_i = L1; /*mark BZP as LOW_LV1*/
11      else
12        bzp_i = L2; /*mark BZP as LOW_LV2*/
13    } else {
14      if (d_ij ≥ 0.92 * D_comm) /*within VERY_HIGH BZP band*/
15        bzp_i = VH; /*mark BZP as VERY_HIGH*/
16      else {
17        if (d_ij − 0.7 * D_comm ≥ 0.3 * D_comm/2) /*more than half comms range*/
18          bzp_i = H1; /*mark BZP as HIGH_LV1*/
19        else
20          bzp_i = H2; /*mark BZP as HIGH_LV2*/
21      }
22    }
23  }
```

Figure 4.7: BZP assignment algorithm. Invoked when non-SH node i overhears RMARK from SH j.

intra-path interference and are outside the interference-zone of the primary path. Using known location information of the source and gateway nodes (i.e. primary, secondary and backup destinations): First, the final destination determines the source quadrant with respect to the primary destination. Next, the preferred quadrants with respect to the primary destination, from which to select the secondary and backup destinations, are determined as shown in Figure 4.10. Let S be the set of gateway nodes that are within communication range of the final destination and in the preferred quadrants. From S, select the secondary and backup destinations

```
1   /*addrOwnSH_i: sector head address of node i*/
2   /*ifz_i: interference-zone marking of node i*/
3   if (addrOwnSH_i == SHj) { /*MIZ1 from own SH*/
4     ifz_i = IFZ1; /*mark as INTEFERENCE_ZONE 1*/
5     if (CheckConditionsForBcastMIZ2( )) /*see line 10*/
6       ComputeDelayAndBcastMIZ2( ); /*see line 22*/
7   }
8
9   /*function to check conditions for MIZ2 broadcast*/
10  CheckConditionsForBcastMIZ2( ) {
11    if ((self not already broadcasted MIZ2) &&
12      (own BZP not VL) &&
13      (own MIZ2 broadcasts overheard limit not reached) &&
14      (own SH not relayed RMARK downstream)) {
15    return TRUE; } else {
16    return FALSE;
17  }
18
19  /*bzp_i: broadcast zone-marker potential marking of node i*/
20  /*delay: random delay for MIZ2 broadcast*/
21  /*function that broadcasts MIZ2 with random delay*/
22  ComputeDelayAndBcastMIZ2( ) {
23    /*the higher the bzp_i, the smaller the offset*/
24    delay = offset + random(0,1) * BCAST_JITTER;
25    BcastsMIZ2(delay);
26  }
```

Figure 4.8: Handle MIZ1 overheard algorithm. Invoked when non-SH node i overhears MIZ1 from SH j.

that are beyond interference range of the primary destination and have the shortest euclidean distances from the source. Finally, the secondary and backup paths are constructed using a technique similar to primary path discovery, except that nodes within interference-zone of primary path (i.e. nodes marked IFZ1 or IFZ2) do not participate in path-discovery.

All markings made by I2MR path discovery are associated with a lifetime and will

```
1   /*addrOwnSH_i: sector head address of node i*/
2   /*addrSH_j: sector head address of node j*/
3   /*countMIZ2_i: counts MIZ2 bcasts overheard by node i*/
4   /*ifz_i: interference zone marking of node i*/
5   if(ifz_i == NULL) /*if unmarked*/
6     ifz_i = IFZ2; /*mark as INTEFERENCE_ZONE 2*/
7   if (addrOwnSH_i == addrSH_j) { /*MIZ2 from same sector*/
8     countMIZ2_i + +; /*increments num. of MIZ2 overheard*/
9     /*use BZP Downgrade Policy for very dense networks*/
10    if (uses BZP Downgrade Policy)
11      DowngradeBZP( ); /*see line 18*/
12    if (CheckConditionsForBcastMIZ2( )) /*see figure 4.8: line 10*/
13      ComputeDelayAndBcastMIZ2( ); /*see figure 4.8: line 22*/
14  }
15
16  /*d_ij: estimated distance between node i and node j*/
17  /*bzp_i: broadcast zone-marker marking of node i*/
18  /*D_comm: communication range of node*/
19  /*function that implements BZP Downgrade Policy*/
20  DowngradeBZP( ) {
21    if (d_ij ≤ D_comm/2) { /*closer to MIZ2 bcast*/
22      switch(bzp_i) { /*downgrades BZP aggressively*/
23      case VH, H1, H2: /*downgrades to LOW_LV2*/
24        { bzp_i = L2; break; }
25      case L1, L2: /*downgrades to VERY_LOW*/
26        { bzp_i = VL; break; }
27      }
28    } else { /*further from MIZ2 bcast*/
29      switch(bzp_i) { /*downgrades BZP less aggressively*/
30      case VH: /*downgrades to HIGH_LV1*/
31        { bzp_i = H1; break; }
32      case H1: /*downgrades to HIGH_LV2*/
33        { bzp_i = H2; break; }
34      case H2: /*downgrades to LOW_LV2*/
35        { bzp_i = L2; break; }
36      }
37    }
38  }
```

Figure 4.9: Handle MIZ2 overheard algorithm. Invoked when non-SH node i overhears MIZ2 from node j.

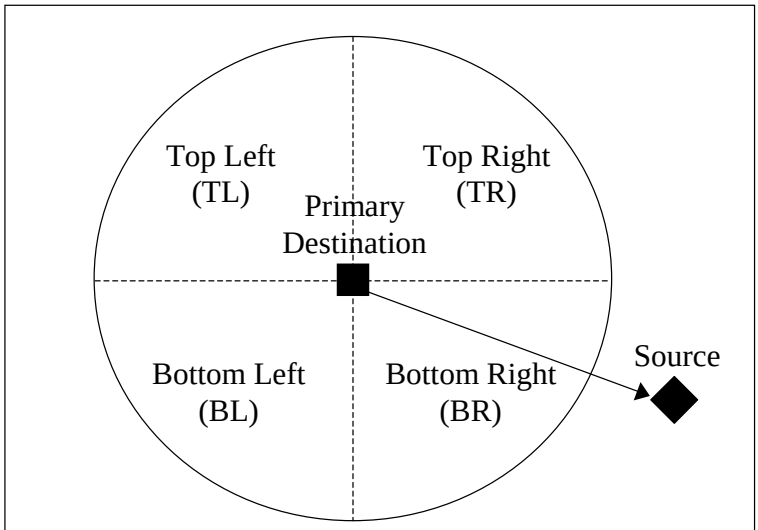

Since source is in bottom right quadrant of primary destination, therefore source quadrant is BR.

Preferred quadrants to select secondary and backup destinations are determined using the table below:

For source quadrant:	Preferred quadrants are:
BR or TL	TR & BL
TR or BL	TL & BR

Figure 4.10: Source quadrant with respect to the primary destination.

be removed once expired. This completes the I2MR path discovery process and the source uses the primary-secondary path-pair concurrently for data transfer, switching to the backup path only when either path fails. Details on how the source loads the active path-pair will be described in the following chapter.

Chapter 5

Congestion Control Scheme for I2MR

Chapter 5 is organized as follow: Section 5.1 defines the problem and gives a brief overview of the congestion control scheme for I2MR. Section 5.2 provides details of the three basic steps of the congestion control scheme for I2MR: 1) Detecting long-term path congestions in Section 5.2.1, 2) Informing the source of long-term path congestions in Section 5.2.2 and 3) Reducing the loading rate of the source in Section 5.2.3.

5.1 Problem Definition and Overview

Section 5.1.1 first defines the problem before Section 5.1.2 gives a brief overview of the proposed congestion control scheme for I2MR.

5.1.1 Problem Definition

After successful I2MR path-discovery, the source starts data transfer to the final destination using the primary-secondary path-pair concurrently, switching to the backup path only when either of the active paths fails. The problem is defined as follow: Given a pair of maximally zone-disjoint paths to be used concurrently for load balancing, load the paths in such a way that long-term congestions do not build-up and the aggregate throughput of the path-pair is maximized.

$$T \propto \frac{1}{I} + \frac{1}{C} + \Phi \tag{5.1}$$

From Equation 5.1, in order to maximize throughput T, the effects of interferences I and the effects due to long-term path congestions C have to be minimized. Φ represents all other factors much less significant than I and C. Therefore, after discovering the path-set that minimizes I (i.e. maximally zone-disjoint shortest paths), the active paths have to be loaded at the highest supportable rate to minimize C.

5.1.2 Scheme Overview

The congestion control scheme for I2MR first loads the paths at an pre-defined initial rate. Intermediate nodes along the active paths detect the build-up of long-term congestions by monitoring their data transmit buffers. In the event that an intermediate node detects long-term congestions, it informs the source to reduce its loading rate. By doing so, the source eventually loads the active paths at the highest possible rate that the paths can support. Therefore, the congestion control scheme can be described in three basic steps as follow:

1. Detecting long-term path congestions.

2. Informing source of long-term path congestions.

3. Reducing loading rate of source.

5.2 Scheme Details

After successful path-discovery, the source starts to load data packets onto the primary-secondary path-pair at initial Src loading rate 1 (i.e. at 1/3 link data rate) as shown in Figure 5.1. The next three sections provide details on the three basic steps of the proposed congestion control scheme.

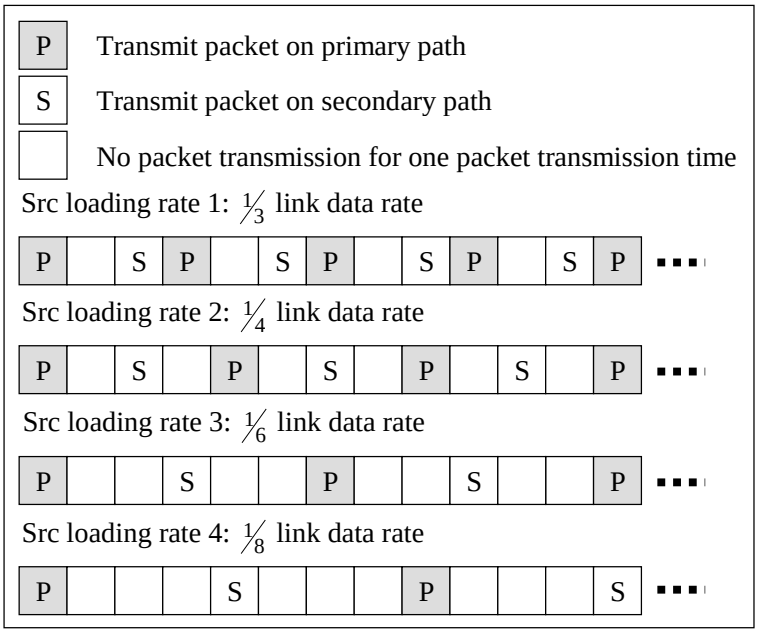

Figure 5.1: Pre-defined loading rates of source in decreasing order.

5.2.1 Detecting Long-term Path Congestions

Intermediate nodes along the active paths detect the on-set of long-term congestions by monitoring the size of their DATA transmit buffers using exponential weighted moving averages (EWMA). Intermediate nodes upon receiving a DATA packet, invoke the algorithm in Figure 5.2 to determine if there is long-term path congestions.

5.2.2 Informing Source of Long-term Path Congestions

In the event that an intermediate node detects the on-set of long-term path congestions, it purges its own DATA transmit buffer of all pending packets. This is to

```
1   /*fCONGSent_i: CONGEST pck sent flag of node i*/
2   /*ewmAvg_i: moving average of data buffer size of node j*/
3   if (CheckForLongTermCongestion( ) && /*see line 21*/
4      fCONGSent_i == FALSE) {
5      /*purges all pending data packets in own data buffer*/
6      PurgeOwnDataBuffer( );
7      /*sends CONGEST control packet to source*/
8      SendCONGPckToSource( );
9      fCONGSent_i = TRUE; /*sets CONGEST pck sent flag*/
10     /*clears fCONGSent_i after predefined interval*/
11     SetTimerToClearCONGSentFlag (interval);
12     ResetEWMAvg( ); /*resets ewmAvg_i to zero*/
13  }
14  RouteDATAPck( ); /*routes data pck to downstream node*/
15
16  /*w_q: weight for calculating moving average*/
17  /*dataBufSize_i: instantaneous data buffer size of node i*/
18  /*EWMA_LIMIT: predefined limit for ewmAvg_i*/
19  /*function that checks if long-term congestion occurs*/*/
20  /*function also updates ewmAvg_i*/
21  CheckForLongTermCongestion( ) {
22     /*exponential weighted moving average calculated*/
23     ewmAvg_i = (1 − w_q) * ewmAvg_i + w_q * dataBufSize_i;
24     if( ewmAvg_i > EWMA_LIMIT )
25        return TRUE; /*long-term congestion*/
26     else
27        return FALSE; /*no long-term congestion*/
28  }
```

Figure 5.2: Handle DATA received algorithm. Invoked when intermediate node i receives a data packet.

reduce the amount of backlogged DATA packets awaiting transmission at the congested node, so as to allow the current DATA packet to be routed with minimal delay. After purging, the congested node sends a CONGEST packet to inform the source of the long-term path congestions. This CONGEST packet is relayed reliably by all the upstream nodes along the active path that the congested node belongs to. Upon successful transmission of the CONGEST packet, the congested node sets a flag, which is cleared after a pre-defined time interval. During this time interval, the congested node will not send any more CONGEST packets to the source. Simultaneously, the congested node resets its EWMA and routes the current DATA packet to its downstream neighbor. All these are summarized in the algorithm as shown in Figure 5.2.

5.2.3 Reducing Loading Rate of Source

The source node upon receiving the CONGEST packet will invoke the algorithm in Figure 5.3 to reduce its loading rate to the next lower pre-defined rate (i.e. either 1/4, 1/6 or 1/8 the link data rate). At 1/8 the link data rate, which is the lowest loading rate possible, the source will not reduce the loading rate any further. Besides reducing the loading rate, the source also suspends packet loading onto the paths for a pre-defined time interval and sets a flag that is cleared after this interval. During this time interval, the source will not react to further CONGEST packets received from intermediate nodes. Eventually, the source will settle at the highest possible

rate that the active paths can support or at the lowest possible loading rate of 1/8 the link data rate. In the event that the loading rate of the source is already at the lowest possible rate (i.e. 1/8 the link data rate) and the source continues to receive CONGEST packets, this implies that the current primary-secondary path-pair is not able to support the lowest loading rate. When the number of CONGEST packets received exceeds a pre-defined limit, the source attempts to switch the congested path with the backup path if possible. Otherwise, the source re-initiates path re-discovery to discover a new path-set. This may also occur when an intermediate node fails or suffers from prolonged outages.

```
1   /*fCONGRx_src: CONGEST received flag of source*/
2   if( fCONGRx_src == FALSE) {
3     StopPckLoading( ); /*stops loading pcks onto active paths*/
4     ReduceSrcLoadingRate ( ); /*see line 15*/
5     fCONGRx(src) = TRUE; /*sets CONGEST received flag*/
6     /*clears fCONGRx(src) after predefined interval*/
7     SetTimerToClearCONGRxFlag( interval );
8     /*starts pck loading onto paths after predefined delay*/
9     /*pcks loaded onto paths using new reduced rate*/
10    ResumePckLoading( delay, currentRate_src );
11  }
12
13  /*currentRate_src: current loading rate of source*/
14  /*function that reduces source loading rate if possible*/
15  ReduceSrcLoadingRate( ) {
16    switch( currentRate_src ) {
17    case SRC_RATE_1: /*1/3 link data rate (initial rate)*/
18      { currentRate_src = SRC_RATE_2; break; }
19    case SRC_RATE_2: /*1/4 link data rate (initial rate)*/
20      { currentRate_src = SRC_RATE_3; break; }
21    case SRC_RATE_3: /*1/6 link data rate (initial rate)*/
22      { currentRate_src = SRC_RATE_4; break; }
23    case SRC_RATE_4: /*1/6 link data rate (initial rate)*/
24      { break; } /*not possible to reduce rate further*/
25    }
26  }
```

Figure 5.3: Handle CONGEST received algorithm. Invoked when source node receives a CONGEST packet.

Chapter 6

Experiments, Results and Discussions

Chapter 6 is organized as follow: Section 6.1 describes the experimental objectives. Section 6.2 describes the simulation model used. Section 6.3 presents and discusses the simulation results obtained.

6.1 Experimental Objectives

First, I2MR is evaluated for different network densities and packet loss rates by comparing the path discovery costs with three other path discovery schemes (i.e. AODV, NDMR and I2MR50). Second, I2MR using congestion control is evaluated for different network densities and packet loss rates by comparing the performances of the

path-sets discovered with AODV, NDMR, I2MR50 and I2MR. Third, the proposed path-set evaluation technique for multipath load balancing is validated. The path discovery schemes under comparison are:

1. ***Ad-hoc On-demand Distance Vector (AODV)***: Basic AODV path discovery where only the destination replies to the first RREQ. Discovers shortest path from source to primary destination. Represents class of unipath on-demand routing schemes. A sample path discovered by AODV is as shown in Figure 6.1.

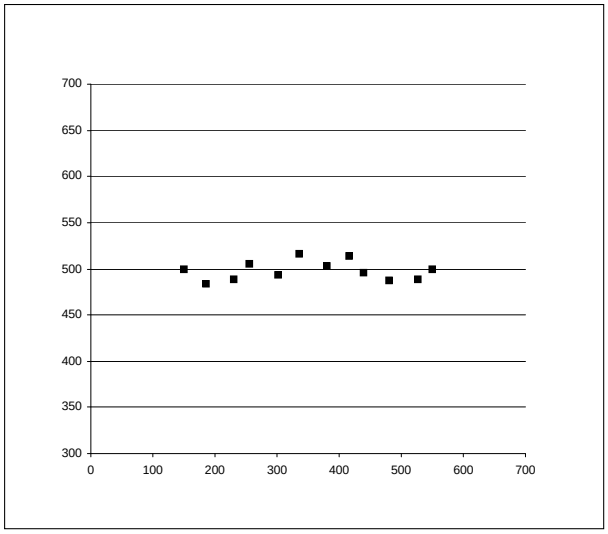

Figure 6.1: Path discovered by AODV.

2. ***Node Disjoint Multi-path Routing (NDMR)*** [13]: Modified AODV path discovery that includes path accumulation feature of DSR. Discovers three node-disjoint shortest paths from source to primary destination. Represents class of multipath routing schemes that modify DSR, using node-disjoint paths. A sample path-set discovered by NDMR is as shown in Figure 6.2.

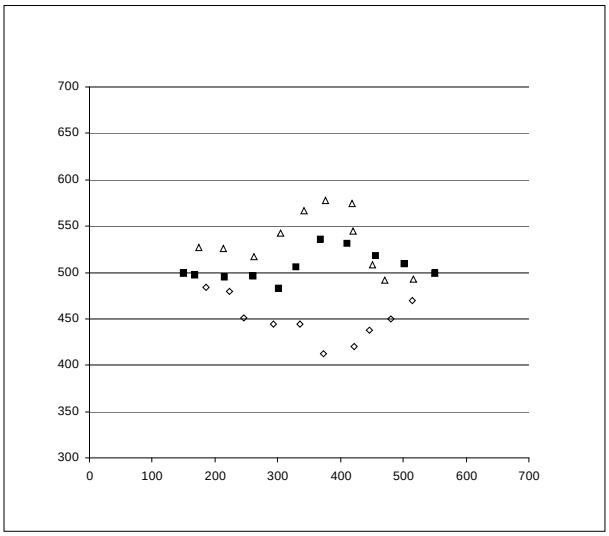

Figure 6.2: Path-set discovered by NDMR.

3. ***I2MR50***: Modified I2MR that discovers three zone-disjoint shortest paths from source to primary, secondary and backup destinations. The secondary and backup paths are physically separated from the primary path by at least communication range (50m). Represents class of multipath routing schemes that discover zone-disjoint paths but assume nodes do not interfere beyond communication range. A sample path-set discovered by I2MR50 is as shown in Figure 6.3.

4. ***I2MR***: The secondary and backup paths are physically separated from the primary path by at least interference range (100m). A sample path-set discovered by I2MR is as shown in Figure 6.4.

5. ***I2MR (CC)***: Using the path-set discovered by I2MR with proposed congestion control scheme (Chapter 5).

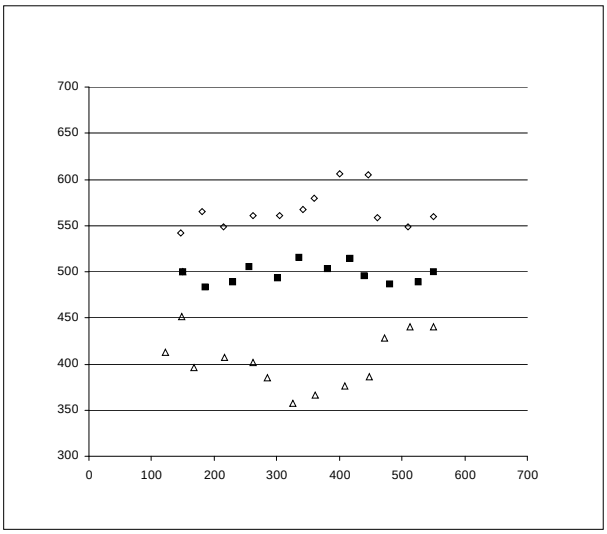

Figure 6.3: Path-set discovered by I2MR50.

In order to compare the path discovery costs of the various path discovery schemes, the following four metrics are used:

1. ***Total path-discovery time***: Total elapsed time for all required paths to be discovered.

2. ***Control packets overheads***: Total number of control packets transmitted by all the nodes in the network for path discovery.

3. ***Control packets overheads in bytes***: Total number of control packets in bytes transmitted by all the nodes in the network for path discovery.

4. ***Total energy consumed for path-discovery***: Total energy consumed by all the nodes in the network for path discovery.

In order to compare the performances of the path-sets discovered by the various schemes, the following four metrics are used:

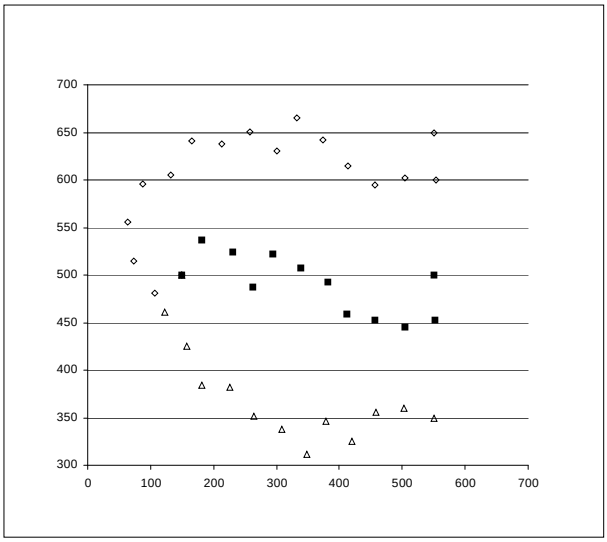

Figure 6.4: Path-set discovered by I2MR.

1. ***Aggregate throughput***: Sum of the individual path throughputs for the active path-pair.

2. ***Average end-to-end delay***: Average delay experienced by packets from source to destinations.

3. ***Total energy consumed***: Total energy consumed by all the nodes for path discovery and data transfer.

4. ***Packet delivery ratio***: Ratio of total packets received at destinations over total packets sent by source.

In order to compare the quality of the path-sets discovered by the various multi-path schemes (i.e. NDMR, I2MR50 and I2MR) and validate the proposed path-set evaluation technique, the following metric is used:

1. ***Total interference correlation factor***: Sum of the path interference correlation factors of all the paths in the active path-set.

6.2 Simulation Model

All the experiments are based on simulations using the GloMoSim network simulator [10]. In all our simulations, static nodes are placed uniformly in a 700mx1000m area, where the area is evenly divided into a number of cells. For a dense network simulated, a total of 7070 nodes are simulated and each cell is of dimension 10mx10m, and for a less dense network, a total of 1836 nodes are simulated and each cell is of dimension 20mx20m. Within each cell, a node is placed randomly. The source node is placed at co-ordinates (150m, 500m) and the destination node of the primary path is placed at co-ordinates (550m, 500m). The destination nodes of the secondary and back-up paths are placed equidistance vertically above and below the destination node of the primary path respectively. A sample network topology is as shown in the Figure 6.5.

The RADIO-ACCNOISE radio model provided by GloMoSim is used for all the simulations. For this model, the radio is able to lock onto a sufficiently strong signal in the presence of interfering signals, up to a certain threshold (i.e. radio capture capability). The radio communication and interference ranges are set to 50m and 100m respectively. This implies that nodes within a circular radius of 50m from a transmitting node are able to receive messages from the node. While nodes further

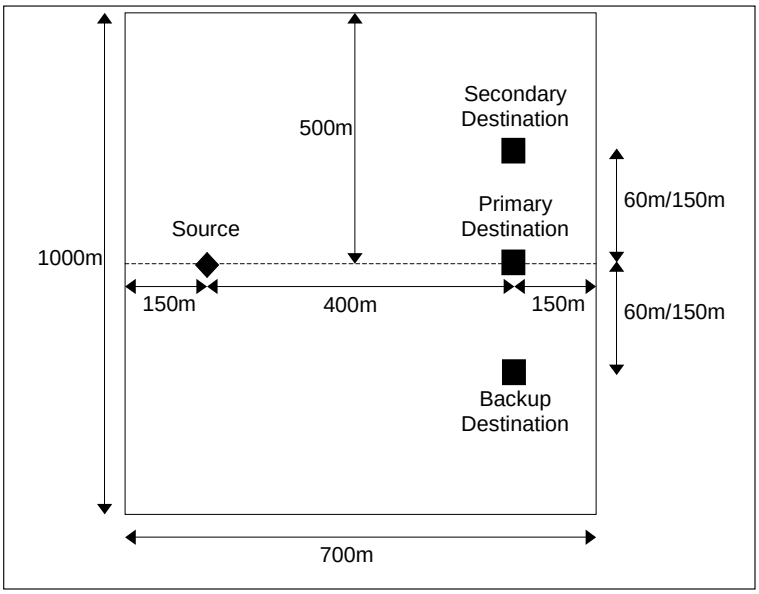

Figure 6.5: Placement of source and destination nodes.

than 50m away, but within a circular radius of 100m from a transmitting node are not able to receive messages from the node correctly, but will be interfered by the transmitting node (i.e. channel will be sensed as busy). The radio parameters as set to model the low-power radio onboard the MICAZ sensor node platform. The radio frequency is set to 2.4GHz and the radio data rate is set to 250Kbps. The energy model of the radio is as follow: The power dissipation of the radio during transmission is 54.0mW, during sensing and reception is 83.1mW and during idle is 24.0mW. The free space propagation model with a threshold cutoff is used as the channel model. In the free space model, the power of a signal attenuates as $\frac{1}{r^2}$, where r is the distance between the communicating nodes. The packet loss rate of the physical channel is modeled using a constant channel bit-error rate (BER), ranging from a BER value of 0 for a no-loss channel to a BER value of $1x10^{-5}$ for a relatively lossy channel.

The IEEE 802.11 Distributed Coordination Function (DCF) model provided by GloMoSim is used as the MAC layer. Physical carrier sensing with exponential backoff is also used. The DATA-ACK two-way hand shaking is used with the maximum re-transmission limit set as two re-tries. This is done to provide a certain degree of reliability while not causing severe congestion due to excessive retransmissions for lossy channels. The RTS/CTS collision avoidance mechanism is turned off to minimize MAC overheads. Data packets are also not fragmented. The MAC layer operates in the promiscuous mode.

A Constant Bit Rate (CBR) source is used to generate a fixed workload for all the simulations. The CBR source sends a total of 40000 data packets of size 1500 bytes from the source node to the destination nodes at a rate close to the radio data rate of 250Kbps (i.e. approximately one data packet every 50.4ms). This ensures that the source node is never idle and always has data packets in its buffer to send. For multipath routing, the source node concurrently uses either the primary-secondary path-pair or the primary-backup path-pair at any one time to transfer data packets to the respective path destination nodes. For scenarios not using congestion control, the source node loads the data packets one after another onto the active path-pair in a round-robin manner. The CBR source waits 20 seconds before starting to send data packets to the destinations, so as to ensure that the path discovery phase is complete.

When the congestion control scheme is used, w_q is set to 0.6, while $EWMA\_LIMIT$

is set to 200 packets and the source waits 5 secs (*delay*) before resuming loading packets onto the active paths at the new reduced rate.

6.3 Simulation Results and Discussions

Each scenario is simulated ten times using different simulation seeds. For AODV, the final results are averaged over ten sets of readings using only the primary path. For NDMR I2MR50, I2MR and I2MR (CC), the final results are averaged over twenty sets of readings, with the first ten obtained using the primary-secondary path-pair and the next ten obtained using the primary-backup path-pair.

Results for the path discovery costs will be presented and discussed first, followed by results for the performances of the path-sets discovered. Finally, results that validate the proposed path-set evaluation technique will be presented and discussed.

First, the results for the path discovery costs are presented and discussed.

Figure 6.6 compares total path discovery time vs. channel BER for both dense and less dense networks. For the dense network in Figure 6.6(a), total path discovery time for I2MR is comparable to both NDMR and I2MR50 and approximately three times more than AODV. For the less dense network in Figure 6.6(b), total path discovery time for I2MR is comparable to NDMR and approximately two and six times more than I2MR50 and AODV respectively. Total path discovery time for I2MR is larger than AODV (i.e. up to six times larger) because up to three paths are discovered for I2MR compared to only one path discovered for AODV. Furthermore, total path

discovery time for I2MR is comparable or at most two times larger than I2MR50 or NDMR even for the less dense network where path discovery is more difficult. Increasing channel BER has little effect for both scenarios.

Figure 6.7 compares total control packets transmitted for path discovery vs. channel BER for both dense and less dense networks. For the dense network in Figure 6.7(a), total control packets transmitted during path discovery for I2MR is comparable to I2MR50 and is approximately 35% and 220% more than NDMR and AODV respectively. For the less dense network in Figure 6.7(b), total control packets transmitted during path discovery for I2MR is comparable to NDMR and is approximately 40% and 250% more than I2MR50 and AODV respectively. For the dense network, total control packets transmitted during path discovery for NDMR is lower than I2MR and I2MR50 because NDMR includes the path accumulation feature of DSR and the route discovery mechanism for DSR uses less control packets than that of AODV, which both I2MR and I2MR50 are derived from. Increasing channel BER has little effect for both scenarios.

Figure 6.8 compares total control bytes transmitted for path discovery vs. channel BER for both dense and less dense networks. For the dense network in Figure 6.8(a), total control packets transmitted during path discovery for I2MR is comparable to I2MR50 and is approximately three times more than AODV. However, total control bytes transmitted during path discovery for I2MR is approximately four times less than NDMR. For the less dense network in Figure 6.8(b), total control packets

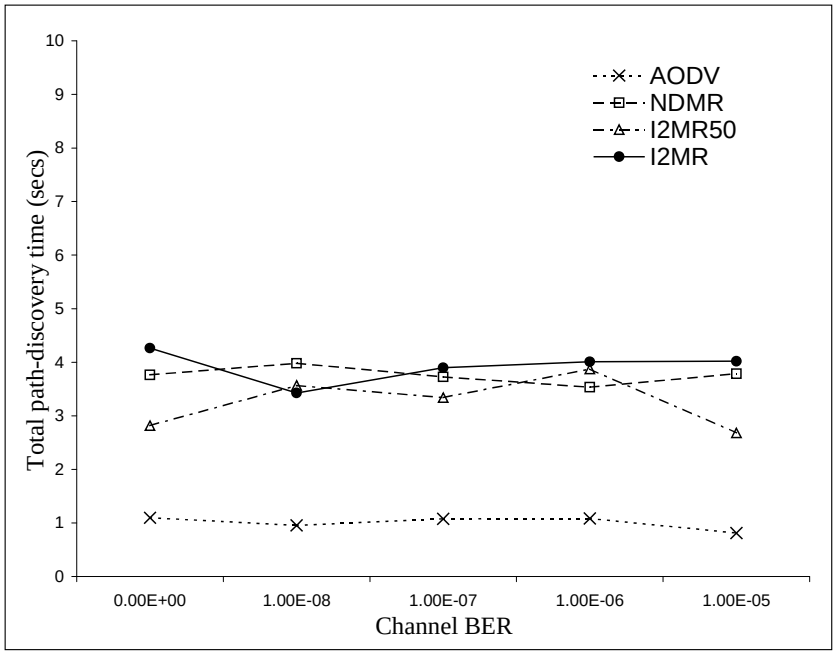

(a)

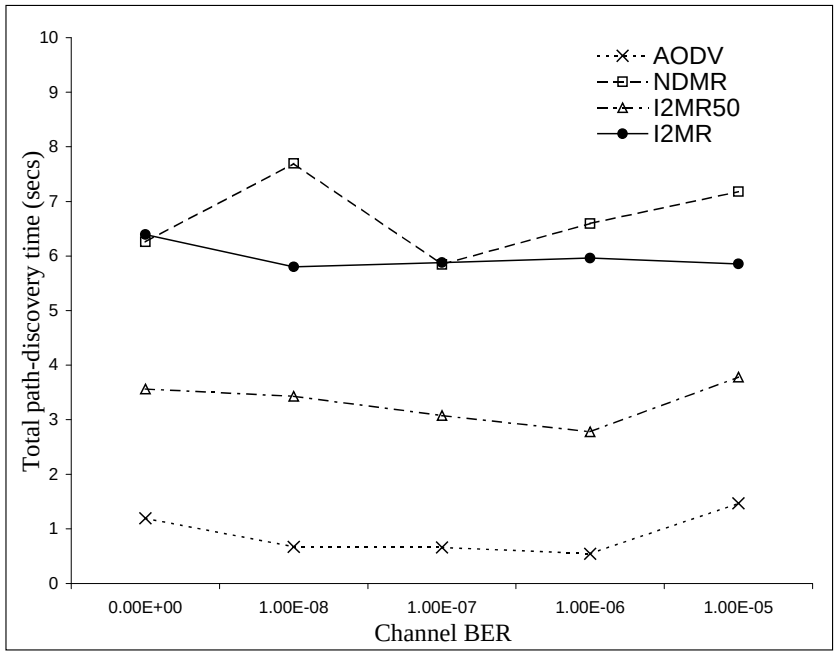

(b)

Figure 6.6: Total path discovery time vs. channel BER for (a) dense network and (b) less dense network.

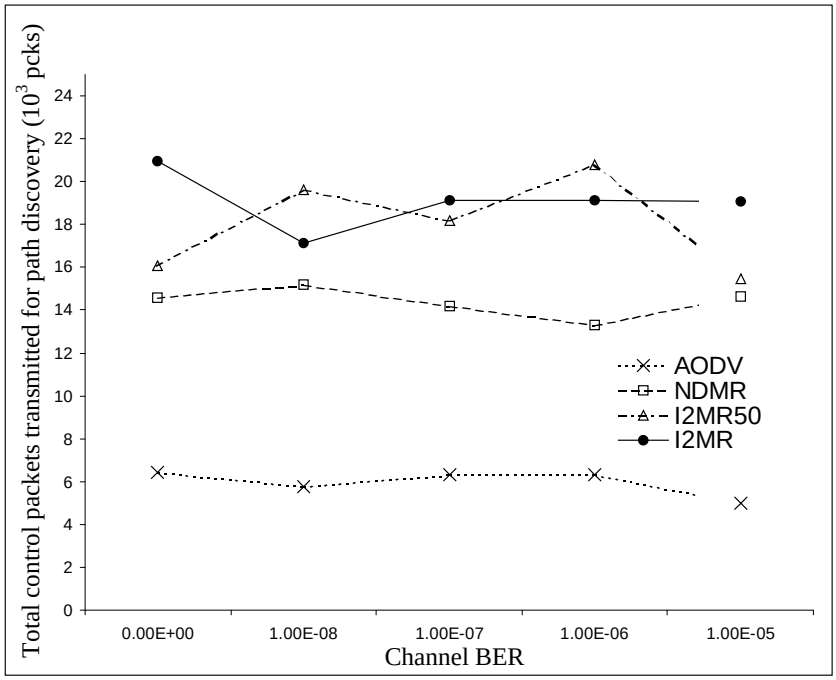

(a)

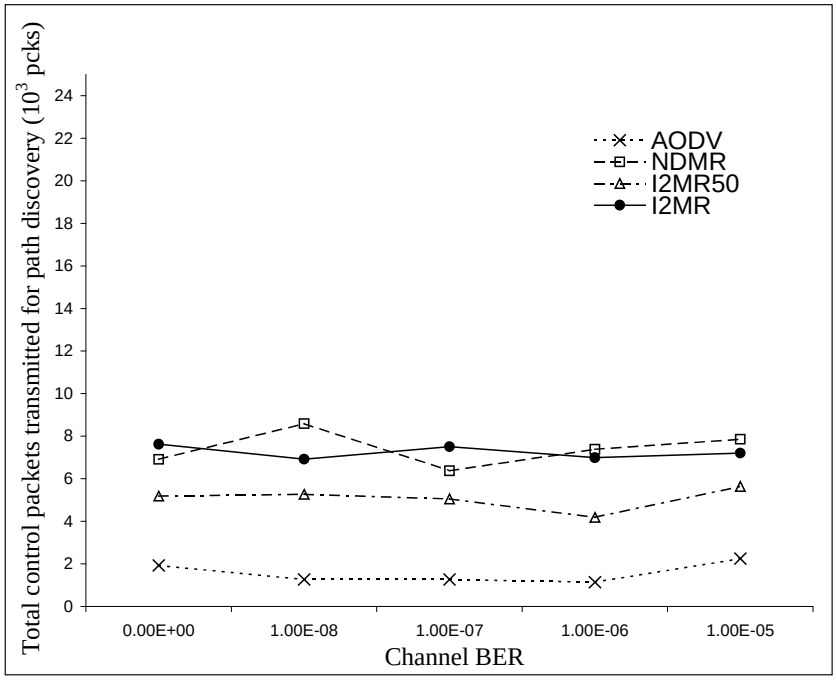

(b)

Figure 6.7: Total control packets transmitted for path discovery vs. channel BER for (a) dense network and (b) less dense network.

transmitted during path discovery for I2MR is approximately two and four times more than I2MR50 and AODV respectively. However, total control bytes transmitted during path discovery for I2MR is approximately five times less than NDMR. An interesting observation made is that although the total control packets transmitted during path discovery for NDMR is comparable or lower than I2MR as shown in Figure 6.7, the total control bytes transmitted during path discovery for NDMR is larger than I2MR. This is because the control packets of NDMR are significantly larger due to path accumulation. Increasing channel BER has little effect for both scenarios.

Figure 6.9 compares total energy consumed for path discovery vs. channel BER for both dense and less dense networks. For the dense network in Figure 6.9(a), I2MR consumes comparable energy as I2MR50 and approximately four times more energy than AODV. However, I2MR consumes approximately 20% lower energy than NDMR. For the less dense network in Figure 6.9(b), I2MR consumes approximately 66% and ten times more energy than I2MR50 and AODV respectively. However, I2MR consumes approximately 20% lower energy than NDMR. During path discovery, I2MR consumes more energy than AODV because more control bytes are transmitted to discover up to 2 more paths as shown in Figure 6.8. However, I2MR consumes lower energy than NDMR because significantly lesser number of control bytes are transmitted as shown in Figure 6.8 due to the significantly smaller control packets. Increasing channel BER has little effect for both scenarios.

Next, the results for the performances of the path-sets are presented and discussed.

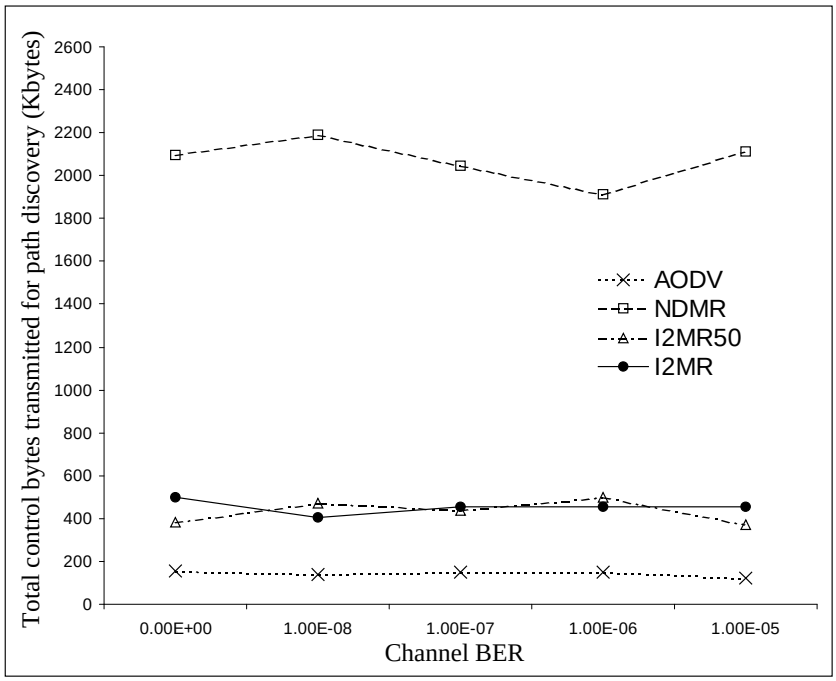

(a)

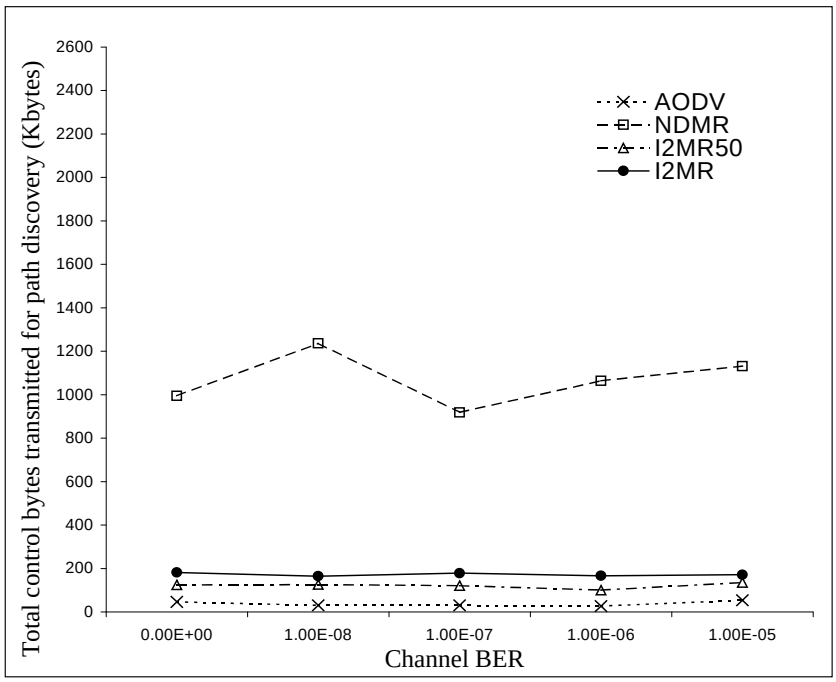

(b)

Figure 6.8: Total control bytes transmitted for path discovery vs. channel BER for (a) dense network and (b) less dense network.

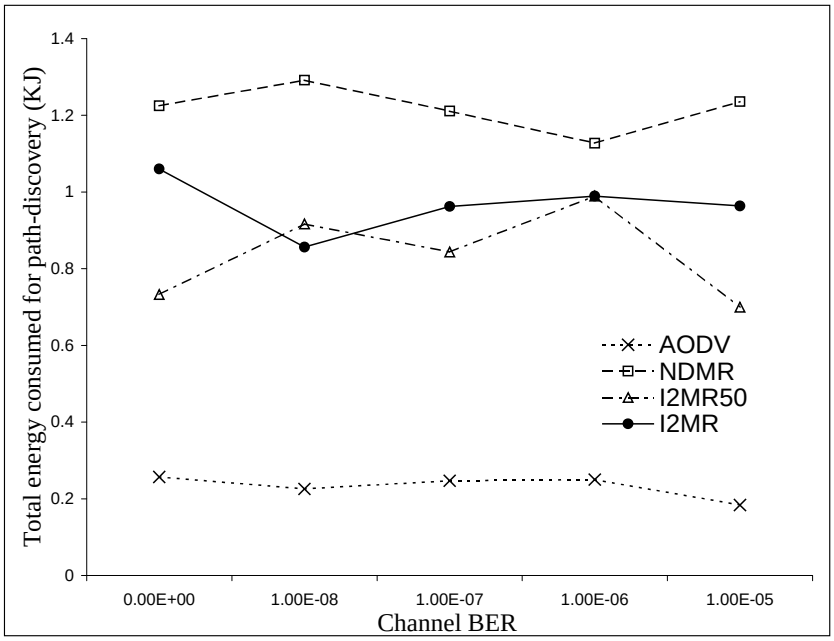

(a)

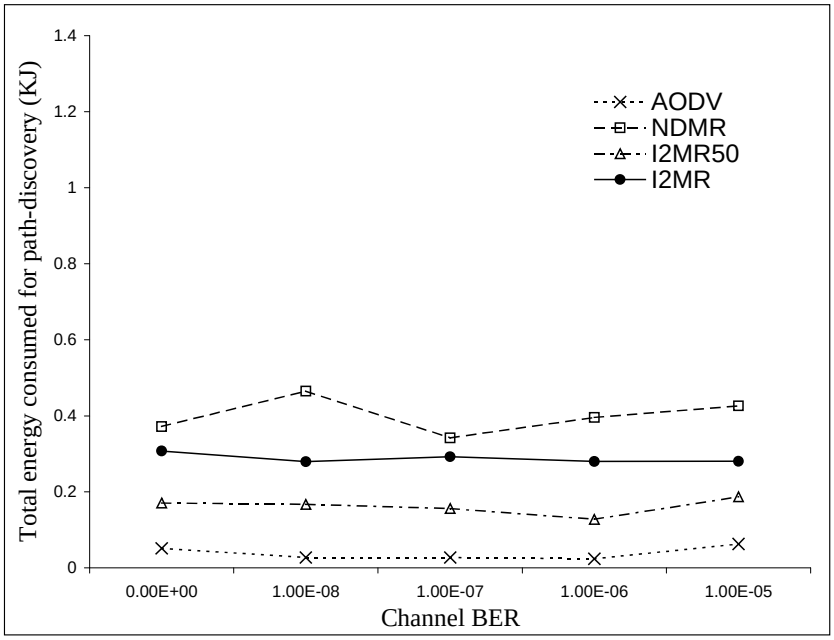

(b)

Figure 6.9: Total energy consumed for path discovery vs. channel BER for (a) dense network and (b) less dense network.

Figure 6.10 compares aggregate throughput vs. channel BER for both dense and less dense networks. For the dense network in Figure 6.10(a) I2MR (CC) achieves the highest aggregate throughputs with approximately 260%, 160%, 110% and 20% gains over AODV, NDMR, I2MR50 and I2MR respectively. For the less dense network in Figure 6.10(b), I2MR (CC) similarly achieves the highest aggregate throughputs with approximately 210%, 140%, 110% and 30% gains over AODV, NDMR, I2MR50 and I2MR respectively. The aggregate throughput for I2MR (CC) is the highest compared to AODV, I2MR50 and NDMR because it uses multipath load balancing with the largest inter-path separation between the active paths, resulting in the lowest inter-path interferences and path congestions. Furthermore, I2MR (CC) loads the active paths at the highest possible rate that can be supported, so as to minimize the effects of long-term congestions, therefore it achieves a higher aggregate throughput than I2MR. For both scenarios, aggregate throughputs decrease gradually with increasing channel BER due to increased packet retransmissions.

Figure 6.11 compares average end-to-end delay vs. channel BER for both dense and less dense networks. For the dense network in Figure 6.11(a), I2MR (CC) achieves the lowest average end-to-end delays compared to AODV, NDMR, I2MR50 and I2MR respectively. For the less dense network in Figure 6.11(b), I2MR (CC) similarly achieves the lowest average end-to-end delays compared to AODV, NDMR, I2MR50 and I2MR. This is because I2MR (CC) uses multipath load balancing with the largest inter-path separation and loads the active paths at the highest possible rate that can

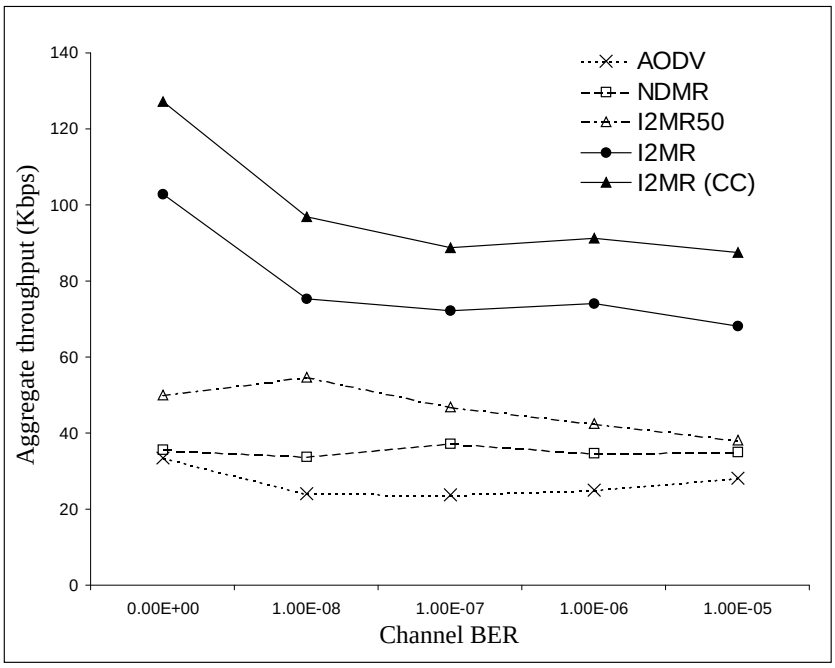

(a)

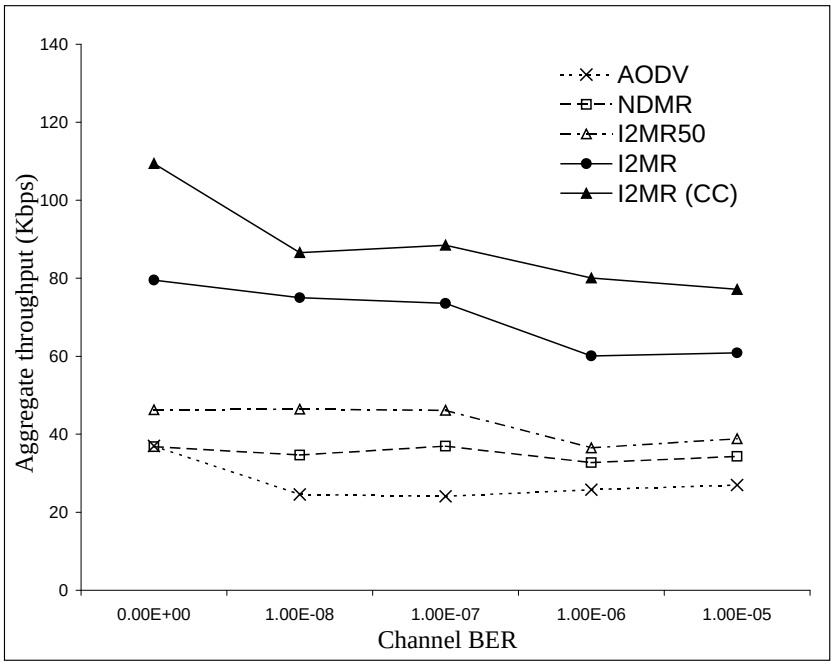

(b)

Figure 6.10: Aggregate throughput vs. channel BER for (a) dense network and (b) less dense network.

be supported by the paths, resulting in the least congested paths for data transfer. Increasing channel BER has little effect for both scenarios.

Figure 6.12 compares total energy consumed vs. channel BER for both dense and less dense networks. For the dense network in Figure 6.12(a), I2MR (CC) consumes comparable energy as AODV and approximately 60%, 50% and 5% lower energy than NDMR, I2MR50 and I2MR respectively. For the less dense network in Figure 6.12(b), I2MR (CC) consumes at most 24% more energy than AODV and approximately 54%, 44% and 4% lower energy than NDMR, I2MR50 and I2MR respectively. Total energy consumed for I2MR (CC) is the lowest compared to NDMR, I2MR50 and I2MR because it uses multipath load balancing with the largest inter-path separation, as total energy consumed decreases with increasing inter-path separation because of lower inter-path interferences. With lower inter-path interferences, lesser packet retransmissions are incurred and data transfer can complete in a shorter time period, hence reducing the total energy consumed. Increasing channel BER has little effect for both scenarios. An interesting observation made is that although the aggregate throughputs for multipath schemes like NDMR, I2MR50, I2MR and I2MR (CC) are higher than the unipath scheme AODV as shown in Figure 6.10, the total energy consumed is larger for multipath schemes compared AODV. There are three possible reasons: Firstly, the total energy consumed to discover a multipath path-set is much higher than that required for a single path as shown in Figure fig:graph energy pd. Secondly,

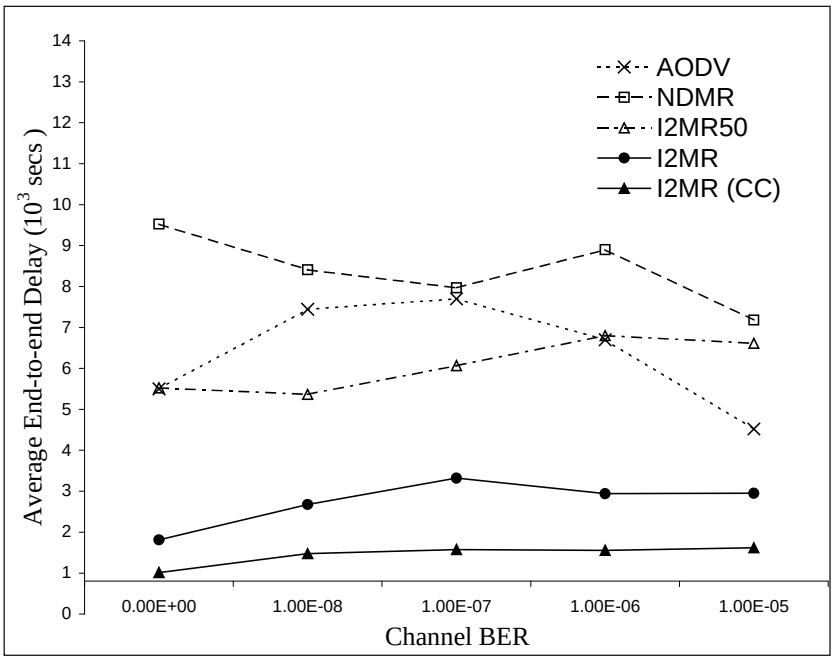

(a)

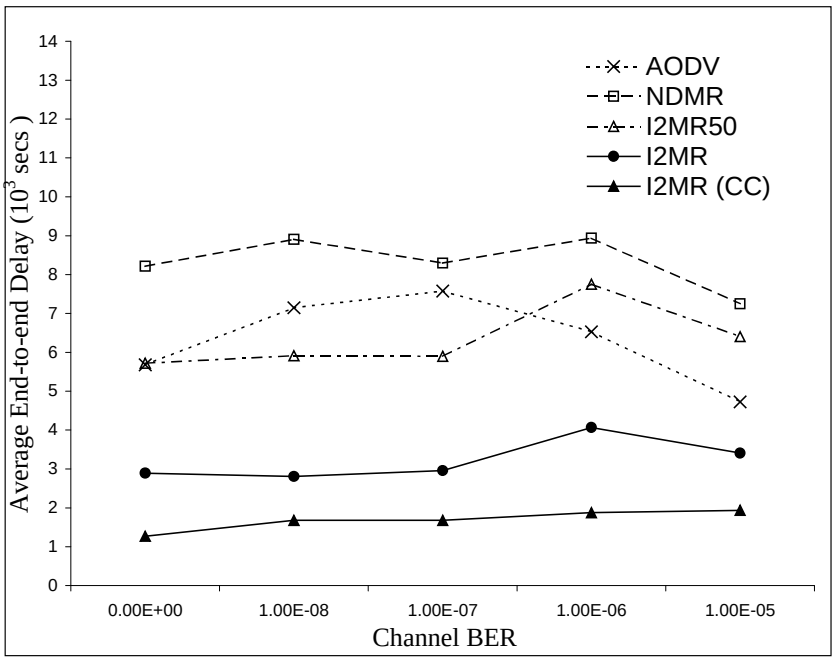

(b)

Figure 6.11: Average end-to-end delay vs. channel BER for (a) dense network and (b) less dense network.

more nodes are involved in data transfer for multipath schemes. Lastly, although aggregate throughputs for multipath schemes are higher than AODV, individual path throughputs may not necessary be higher than AODV.

Figure 6.13 compares packet delivery ratio vs. channel BER for both dense and less dense networks. There is no significant degradation in performance for the less dense network and packet delivery ratios remain relatively constant as BER increases until it reaches 1.0E-5, where a slight drop is observed. The packet delivery ratios for I2MR, I2MR50 and AODV are comparable and very close to 1, while packet delivery ratios for NDMR and I2MR (CC) are slightly lower. For the case of NDMR, packets are lost due to severe inter-path interferences, resulting in the retransmission limits for intermediate nodes along the paths to be exceeded due to congestions. For the case of I2MR (CC), packets are purged at the initial stages of data transfer when the source reduces its loading rate when long-term congestions occur. Once the source eventually settles down at the highest possible rate supportable by the active paths, minimal packet losses are observed.

Lastly, the results that validates the proposed path-set evaluation technique are presented and discussed.

Figure 6.14 compares total interference correlation factor vs. channel BER for both dense and less dense networks. For the dense network in Figure 6.14(a), I2MR has the lowest total interference correlation factor, followed by I2MR50 and then NDMR, which has the highest total interference correlation factor. For the less dense

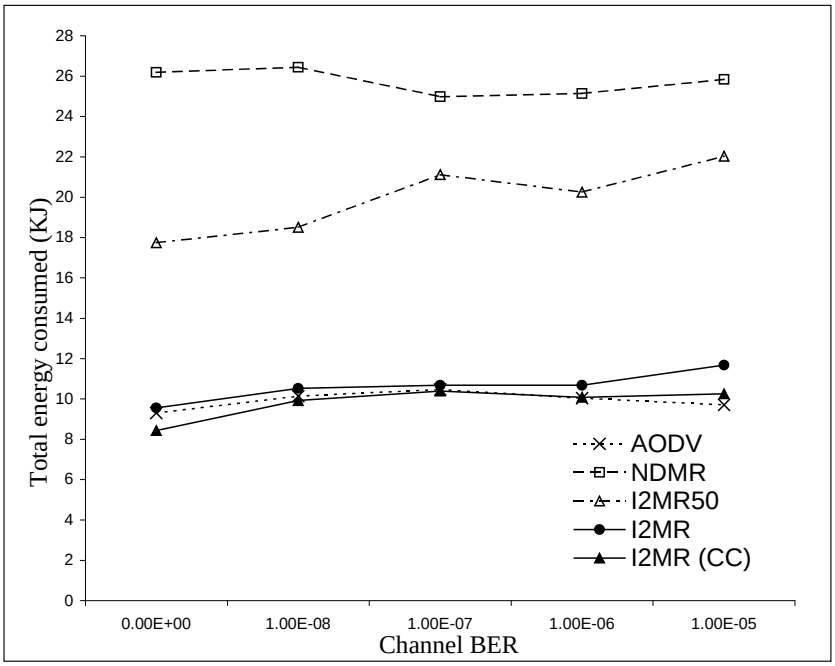

(a)

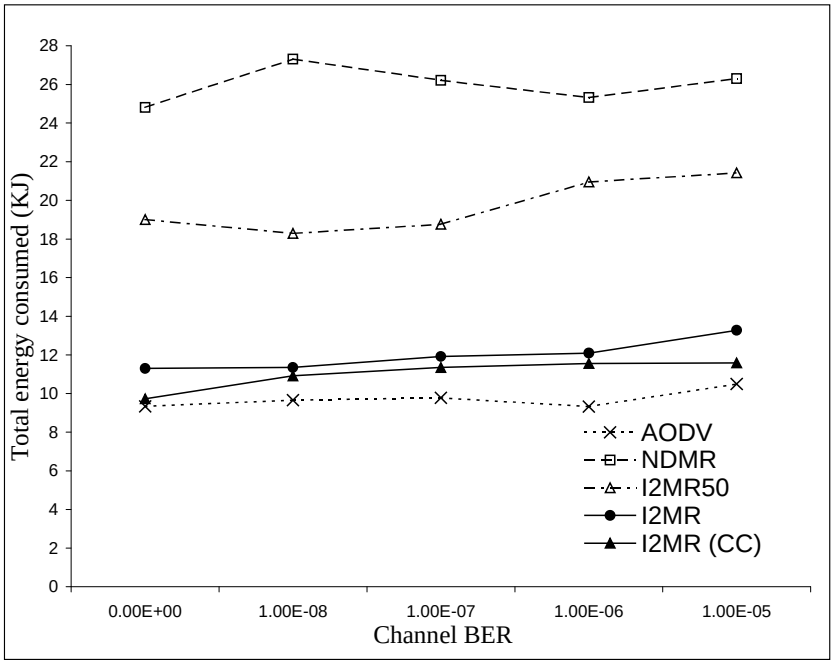

(b)

Figure 6.12: Total energy consumed vs. channel BER for (a) dense network and (b) less dense network.

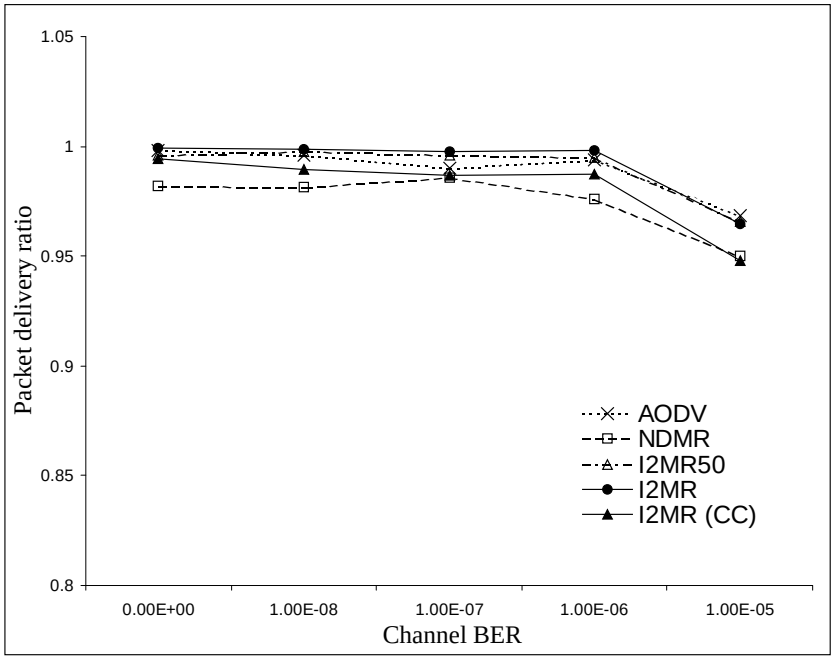

(a)

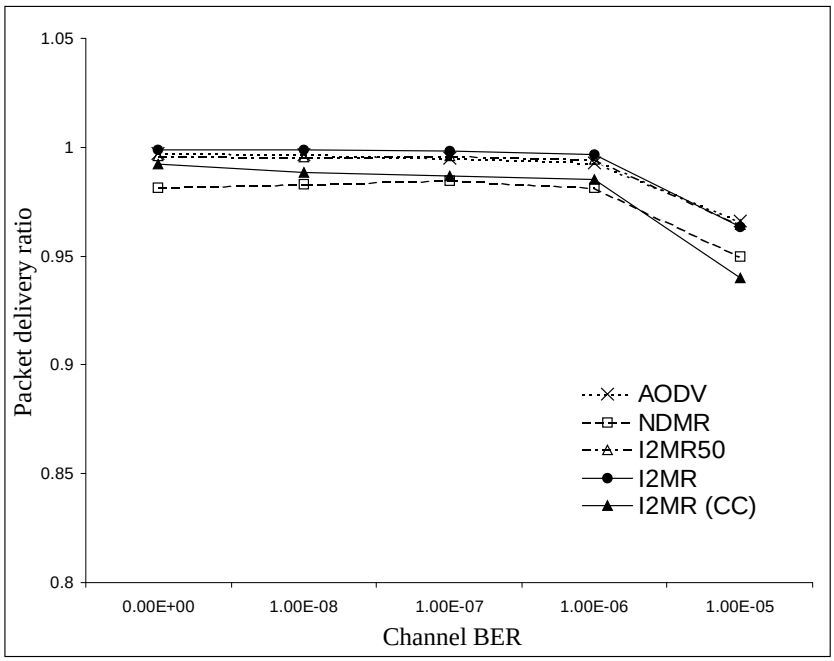

(b)

Figure 6.13: Packet delivery ratio vs. channel BER for (a) dense network and (b) less dense network.

network in Figure 6.14(b), I2MR also has the lowest total interference correlation factor, followed by I2MR50 and then NDMR, which has the highest total interference correlation factor. Comparing I2MR, I2MR50 and NDMR, since I2MR achieves the lowest total interference correlation factor, followed by I2MR50 and then NDMR, therefore the aggregate throughput achieved by the path-set discovered by I2MR is expected to be the highest, followed by I2MR50 and then NDMR, which is expected to achieve the lowest aggregate throughput. This is indeed the case as shown in Figure 6.10.

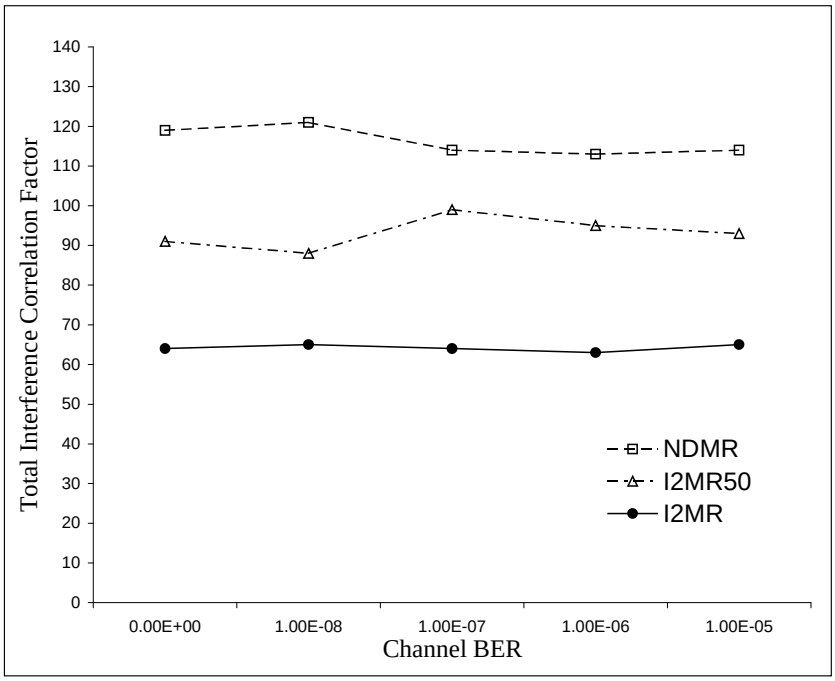

(a)

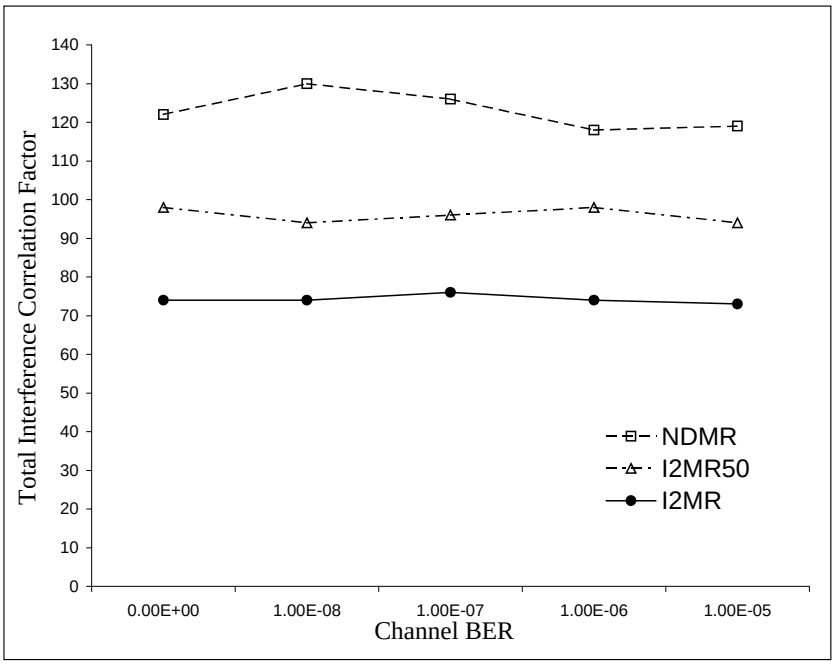

(b)

Figure 6.14: Total interference correlation factor vs. channel BER for (a) dense network and (b) less dense network.

Chapter 7

Conclusion, Limitations and Future Works

Chapter 7 is organized as follow: Section 7.1 summarizes the experimental results obtained and then conclude. Section 7.2 discusses possible limitations and suggests future works.

7.1 Summary of Results and Conclusion

Comparing the path discovery costs for I2MR, I2MR50, NDMR and AODV: The total path discovery time, total control bytes transmitted and total energy consumed during path discovery for I2MR is at least comparable or if not better than NDMR and not prohibitively larger than AODV and I2MR50. Although I2MR may transmit

more control packet than NDMR, but the size of the control packets for NDMR is significantly larger than I2MR, resulting in NDMR consuming more energy than I2MR during path discovery.

Comparing the path-set performances for I2MR (CC), I2MR, I2MR50, NDMR and AODV: I2MR using congestion control (i.e. I2MR (CC)) achieves the highest throughput with up to 260%, 160%, 110% and 20% gains over AODV, NDMR, I2MR50 and I2MR respectively and the lowest average end-to-end delays. Total energy consumed by I2MR (CC) is also the lowest among all the multipath schemes, up to 60%, 50% and 5% lower than NDMR, I2MR50 and I2MR respectively. When compared with AODV, I2MR (CC) consumes comparable or at most 24% more energy. I2MR (CC) also achieves acceptable packet delivery ratios with most packets losses occurring only in the initial stages of data transfer due to purging.

Comparing the quality of the path-sets for I2MR, I2MR50 and NDMR: The path-set discovered by I2MR has the lowest total interference correlation factor (i.e. highest quality), followed by I2MR50 then NDMR, which has the highest total interference correlation factor (i.e. lowest quality).

Based on the results obtained, it can be concluded that:

1. The proposed path-set evaluation technique for multipath load balancing is able capture both the effects of inter- and intra-path wireless interferences, while assuming that nodes may interfere beyond their communication ranges. Furthermore, the derived total interference correlation factor metric can be used

to evaluate the quality of a path-set discovered for multipath load balancing.

2. The proposed I2MR protocol is able to significanly increase throughput by discovering and using maximally zone-disjoint shortest paths for load balancing, while requiring minimal localization support and incurring low overheads. Furthermore, directional antennas are not used and nodes may interfere up to twice their communication ranges.

3. The propose congestion control scheme is able further increase throughput by loading the active paths at the highest possible rate that can be supported, so as to minimize long-term path congestions.

7.2 Limitations and Future Works

A possible limitation of the proposed I2MR protocol is that the wireless interferences between neighboring path-sets used by different source-final destination pairs require the deployment of these pairs to be suitably spaced-out.

For future works, we hope to extend the proposed I2MR protocol to take into account the effects of inter path-set interferences, so as to ease the deployment of the WSN.

Bibliography

[1] Stephen Mueller, Rose P. Tsang, and Dipak Ghosal. Multipath routing in mobile ad hoc networks: Issues and challenges. In *MASCOTS Tutorials*, pages 209–234, 2003.

[2] E. P. C. Jones, M. Karsten, and P. A. S. Ward. Multipath load balancing in multi-hop wireless networks. *Wireless And Mobile Computing, Networking And Communications, 2005. (WiMob'2005), IEEE International Conference on*, 2:158–166 Vol. 2, 2005.

[3] Kamal Jain, Jitendra Padhye, Venkata N. Padmanabhan, and Lili Qiu. Impact of interference on multi-hop wireless network performance. In *MobiCom '03: Proceedings of the 9th annual international conference on Mobile computing and networking*, pages 66–80, New York, NY, USA, 2003. ACM Press.

[4] Shree Murthy and J. J. Garcia-Luna-Aceves. An efficient routing protocol for wireless networks. *Mob. Netw. Appl.*, 1(2):183–197, 1996.

[5] Charles E. Perkins and Pravin Bhagwat. Highly dynamic destination-sequenced distance-vector routing (dsdv) for mobile computers. In *SIGCOMM '94: Proceedings of the conference on Communications architectures, protocols and applications*, pages 234–244, New York, NY, USA, 1994. ACM Press.

[6] Charles E. Perkins and Elizabeth M. Royer. Ad-hoc on-demand distance vector routing. In *WMCSA '99: Proceedings of the Second IEEE Workshop on Mobile Computer Systems and Applications*, page 90, Washington, DC, USA, 1999. IEEE Computer Society.

[7] David B. Johnson and David A. Maltz. Dynamic source routing in ad hoc wireless networks. In Imielinski and Korth, editors, *Mobile Computing*, volume 353. Kluwer Academic Publishers, 1996.

[8] Vivek K. Goyal. Multiple description coding: Compression meets the network. *IEEE Signal Processing Magazine*, 18(5):74–93, September 2001.

[9] Y. Wang, S. Panwar, S. Lin, and S. Mao. Wireless video transport using path diversity: multiple description vs. layered coding. In *Proc. IEEE Int. Conf. on Image Proc., Rochester, USA*, September 2002.

[10] Xiang Zeng, Rajive Bagrodia, and Mario Gerla. Glomosim: a library for parallel simulation of large-scale wireless networks. In *PADS '98: Proceedings of the twelfth workshop on Parallel and distributed simulation*, pages 154–161, Washington, DC, USA, 1998. IEEE Computer Society.

[11] Mario Gerla and Kaixin Xu. Multimedia streaming in large-scale sensor networks with mobile swarms. *SIGMOD Rec.*, 32(4):72–76, 2003.

[12] Sung-Ju Lee and Mario Gerla. Aodv-br: Backup routing in ad hoc networks. In *Proceedings of the IEEE Wireless Communications and Networking Conference (WCNC 2000)*, Chicago, IL, Sepember 2000.

[13] Xuefei Li and Laurie Cuthbert. A reliable node-disjoint multipath routing with low overhead in wireless ad hoc networks. In *MSWiM '04: Proceedings of the 7th ACM international symposium on Modeling, analysis and simulation of wireless and mobile systems*, pages 230–233, New York, NY, USA, 2004. ACM Press.

[14] M. Marina and S. Das. On-demand multipath distance vector routing in ad hoc networks. In *ICNP '01: Proceedings of IEEE International Conference on Network Protocols*, pages 14–23, 2001.

[15] Jinyang Li, Charles Blake, Douglas S. J. De Couto, Hu Imm Lee, and Robert Morris. Capacity of ad hoc wireless networks. In *Mobile Computing and Networking*, pages 61–69, 2001.

[16] Marc R. Pearlman, Zygmunt J. Haas, Peter Sholander, and Siamak S. Tabrizi. On the impact of alternate path routing for load balancing in mobile ad hoc networks. In *MobiHoc '00: Proceedings of the 1st ACM international symposium on Mobile ad hoc networking & computing*, pages 3–10, Piscataway, NJ, USA, 2000. IEEE Press.

[17] P. Pham and S. Perreau. Multi-path routing protocol with load balancing policy in mobile ad hoc network. *Mobile and Wireless Communications Network, 2002. 4th International Workshop on*, pages 48–52, 2002.

[18] Ren Xiuli and Yu Haibin. A novel multipath disjoint routing to support ad hoc wireless sensor networks. In *ISORC '06: Proceedings of the Ninth IEEE International Symposium on Object and Component-Oriented Real-Time Distributed Computing (ISORC'06)*, pages 174–178, Washington, DC, USA, 2006. IEEE Computer Society.

[19] Kui Wu and Janelle Harms. Performance study of a multipath routing method for wireless mobile ad hoc networks. In *MASCOTS '01: Proceedings of the Ninth International Symposium in Modeling, Analysis and Simulation of Computer and Telecommunication Systems (MASCOTS'01)*, page 99, Washington, DC, USA, 2001. IEEE Computer Society.

[20] Gang Zhou, Tian He, Sudha Krishnamurthy, and John A. Stankovic. Impact of radio irregularity on wireless sensor networks. In *MobiSys '04: Proceedings of the 2nd international conference on Mobile systems, applications, and services*, pages 125–138, New York, NY, USA, 2004. ACM Press.

[21] Nam T. Nguyen, An-I Andy Wang, Peter Reiher, and Geoff Kuenning. Electric-field-based routing: a reliable framework for routing in manets. *SIGMOBILE Mob. Comput. Commun. Rev.*, 8(2):35–49, 2004.

[22] Siuli Roy, Somprakash Bandyopadhyay, Tetsuro Ueda, and Kazuo Hasuike. Multipath routing in ad hoc wireless networks with omni directional and directional antenna: A comparative study. In *IWDC '02: Proceedings of the 4th International Workshop on Distributed Computing, Mobile and Wireless Computing*, pages 184–191, London, UK, 2002. Springer-Verlag.

[23] Siuli Roy, Dola Saha, S. Bandyopadhyay, Tetsuro Ueda, and Shinsuke Tanaka. A network-aware mac and routing protocol for effective load balancing in ad hoc wireless networks with directional antenna. In *MobiHoc '03: Proceedings of the 4th ACM international symposium on Mobile ad hoc networking & computing*, pages 88–97, New York, NY, USA, 2003. ACM Press.